

# **Impact of pathogen intrusion in water distribution network under sustained low pressure conditions**

*Master of Science Thesis in Infrastructure and Environmental Engineering*

VERONICA FALK  
MICHAEL ODHIAMBO

Department of Architecture and Civil Engineering  
*Water Environment Technology*  
CHALMERS UNIVERSITY OF TECHNOLOGY  
Master's Thesis ACEX30  
Göteborg, Sweden 2021



MASTER'S THESIS ACEX30

# **Impact of pathogen intrusion in water distribution network under sustained low pressure conditions**

*Master's Thesis in the Master's Programme Infrastructure & Environmental Engineering*

VERONICA FALK  
MICHAEL ODHIAMBO

Department of Architecture and Civil Engineering  
*Division of Water Environment Technology*  
CHALMERS UNIVERSITY OF TECHNOLOGY  
Göteborg, Sweden 2021



Impact of pathogen intrusion in water distribution network under sustained low pressure conditions

*Master's Thesis in the Master's Programme Infrastructure & Environmental Engineering*

VERONICA FALK

MICHAEL ODHIAMBO

© VERONICA FALK & MICHAEL ODHIAMBO, 2021

Examensarbete ACEX30

Institutionen för arkitektur och samhällsbyggnadsteknik  
Chalmers tekniska högskola, 2021

Department of Architecture and Civil Engineering  
Water Environment Technology  
Chalmers University of Technology  
SE-412 96 Göteborg  
Sweden  
Telephone: + 46 (0)31-772 1000

Department of Architecture and Civil Engineering  
Göteborg, Sweden, 2021



Impact of pathogen intrusion in water distribution network under sustained low pressure conditions

*Master's thesis in the Master's Programme Infrastructure & Environmental Engineering*

VERONICA FALK

MICHAEL ODHIAMBO

Department of Architecture and Civil Engineering  
Division of Water Environment Technology  
Chalmers University of Technology

## **ABSTRACT**

Drinking water distribution networks across the world are of high average age, and in many cases in poor condition due to delayed or inadequate maintenance. These conditions in combination with regular water distribution network pressure losses present significant challenges for water utilities in providing safe water. This study presents an assessment of human health risk resulting from pathogen intrusion in a water distribution network (WDN) under sustained low pressure events. Two low pressure causing events, a pump failure, and extreme water use through a fire hydrant, were simulated.

EPANET water quality/hydraulic model was used for simulating transport and fate of pathogen intrusion in a WDN under sustained low pressure conditions. Quantitative microbial risk assessment (QMRA) was used for determining the infection risks for the people exposed. The areas with sustained low negative pressure were identified as vulnerable zones where the distribution of pathogens was investigated using EPANET and risk determined with QMRA.

The results indicate that 2.3% of the network was at risk of pathogen intrusion in the event of a pump failure while 2.9% of the network could be at risk from emergency fire events. The QMRA result indicates a 100% probability of infection of the population exposed during the short event time. The factors that influence pathogen intrusion and hence the risk were found to be the duration and magnitude of the low pressure event, affected section length, and size of leakage.

Overall, the infection risks exceeded the “United States Environmental Protection Agency's” recommended limit of  $10^{-6}$  persons infected per day hence mitigation measures were necessary to minimize the risks in case of these events. Measures that reduce the exposure to consumers, such as pressure and water quality management, leak repair, and isolation of affected areas, were considered primary measures for reducing risks. Sensors were thus proposed to act as early warning systems in the event of pressure or quality change.

Keywords: EPANET, QMRA, Water Distribution Network, Demand Driven Analysis (DDA), Pressure Driven Analysis (PDA), Risk Analysis, low pressure, Water quality, simulation



Effekten av patogenintrång i ett vattendistributionsnät under långvariga lågtrycksförhållanden

*Examensarbete inom masterprogrammet Infrastruktur och Miljöteknik*

VERONICA FALK

MICHAEL ODHIAMBO

Institutionen för arkitektur och samhällsbyggnadsteknik  
Avdelningen för Vatten Miljö Teknik  
Chalmers tekniska högskola

## **SAMMANFATTNING**

Distributionssystem för dricksvatten världen över är gamla och i många fall i dåligt skick på grund av försenat och bristande underhåll. Begränsningar som dessa i kombination med regelbundet tryckfall i ledningsnäten utgör en betydande utmaning för produktion av säkert dricksvatten. Denna studie presenterar en bedömning av hälsoriskerna för konsumenten på grund av intrång av patogener i ledningarna som resultat av lågt tryck. Studien inkluderar två vanligt förekommande scenarion, det ena är pumpfel och det andra är extremt vattenuttag.

Modelleringsverktyget EPANET användes för att analysera transport och förekomst av patogener i ledningsnätet. Kvantitativ Mikrobiologisk Riskanalys (QMRA) användes för att bedöma infektionsrisken för konsumenten vid förekomst av patogenhalten som ett resultat av intrånget. De områden där trycket i noderna var mindre än noll identifierades som lågtrycksområden där fördelningen av patogener analyserades med EPANET och QMRA användes för att bedöma den slutliga risken.

Resultatet indikerade att risken för patogenintrång för trycksfallscenariot fanns för 2.3% av det totala analyserade nätverket medan det för vattenuttagsscenariot var 2.9%. QMRA resultatet visar risken för infektion för båda scenariona är 100% för de personer som exponeras under den relativt korta exponeringstiden. Det som bedöms påverka inflödet av patogener och därmed risken för konsumenten är låg-trycks scenariots storlek och varaktighet, längden på nätet som påverkas och storlek på läckaget.

Slutligen visar det att infektionsrisken överstiger amerikanska miljöförvaltningsmyndighetens rekommendation  $10^{-6}$  personer som infekteras dagligen, varför åtgärder behöver vidtas för att minimera riskerna för dessa typer av event. För att mildra effekterna ansågs att minska risken för exponering vara den bästa åtgärden, och det föreslås användning av sensorer som ett tidigt varningssystem.

Nyckelord: EPANET, QMRA, Vattendistributionssystem, Trycksdriven analys (PDA), Behovsdriven analys (DDA), Riskanalys, Lågtryck, Vattenkvalitet, Simulering

## ACKNOWLEDGEMENT

We are grateful to Chalmers University of Technology for ensuring our studies stayed on schedule despite the hard times due to the COVID-19 pandemic.

We extend our heartfelt gratitude to Prof. Thomas Petterson, our supervisor, for the guidance and support he has offered throughout the project. He was very instrumental in helping us piece together ideas that have become the basis of this study. We have immensely benefitted from his understanding of this topic and directions when we hit rock bottom.

To our examiner, Associate Prof. Ekaterina Sokolova, we are grateful for the insights in the project, guidance, and help in the acquisition of materials and data that have been instrumental in this project. We will always treasure the support and the feedback you have accorded us in shaping the path for this project.

We are greatly indebted to Victor Vinas for his time, prompt response to our questions, and great insights in modeling and QMRA. We were able to overcome obstacles with his guidance and motivation.

Much appreciation to the staff at the water utility south of Sweden for the data and the model we used in our studies. It gave us insight into the real challenges faced by the real water distribution networks.

To our families, we thank you for the sacrifices you have made to see us this far. You have been a source of joy, inspiration, and comfort. You have always been there for us when we needed you most.

Finally, I (Michael) wish to extend my heartfelt gratitude to the *Swedish Institute* (SI) for the *Swedish Institute Scholarship for Global professional (SISGP)*, without which this master's study would not have been possible. The last two years have been amazing in integrating into the Swedish culture. Through the *Network for Future Global leaders (NFGL)*, I have interacted with many scholars from various nationalities and gained an overview of world cultures.

Gothenburg, May 2021

Veronica Falk and Michael Odhiambo

## Contents

ABSTRACT	I
SAMMANFATTNING	I
ACKNOWLEDGEMENT	II
CONTENTS	III
LIST OF TABLES	VI
LIST OF FIGURES	VII
1. INTRODUCTION	1
1.1. Background	2
1.2. Aim	3
1.3. Specific objectives	3
1.4. Limitations	4
2. HYDRAULIC MODELING AND QMRA	5
2.1. Applications of hydraulic modeling and QMRA	5
2.1.1. Main pipeline repair	6
2.1.2. Biofilm	8
2.1.3. Intrusion	8
2.1.4. Multiple contamination events	9
2.1.5. Crossflow connection	10
2.2. Hydraulic and QMRA modeling tools	11
2.2.1. Mike Urban+	11
2.2.2. EPANET 2.2	13
2.2.3. EPANET MSX	19
2.2.4. Water network management (Aquis).	19
2.2.5. Quantitative Microbial Risk Assessment (QMRA)	19
2.3. Pathogens	26
2.3.1. Indicator organisms	26
2.3.2. Cryptosporidium	26
2.3.3. Norovirus	27
2.3.4. Campylobacter	27
2.3.5. The ratio between <i>E. coli</i> and pathogens	27
2.4. Summary of Hydraulic modeling and QMRA	28
3. METHOD	29
3.1. Study area description	29

3.2. Modeling process	30
3.3. Hydraulic simulation	30
3.4. Scenarios	31
3.4.1. Scenario 1 – Normal operation conditions	31
3.4.2. Scenario 2 – Low pressure condition (Malfunctioning pump(s))	32
3.4.3. Scenario 3 – Fire emergency water supply	32
3.5. Pathogen intrusion	32
3.5.1. Intrusion volume	32
3.5.2. Pathogen concentration	34
3.6. Modeling Water quality with EPANET	35
3.7. Estimating health risks with QMRA	36
4. RESULTS	38
4.1. Hydraulic characteristic of normal operation conditions	38
4.2. Hydraulic characteristic of low pressure conditions	39
4.3. Low/Negative pressure zoning	40
4.4. Pathogen intrusion rate into the WDN	41
4.5. Pathogen distribution in the WDN during sustained low pressure events	42
4.6. Risk analysis in QMRA	44
5. DISCUSSION	45
5.1. Hydraulic modeling under sustained low pressure conditions	45
5.2. Spatial distribution of zones vulnerable to intrusion	45
5.3. Contaminant intrusion	46
5.4. Water Quality-Fate and transport of pathogens	47
5.5. Health risk characterization (QMRA)	47
5.6. Mitigation measures	48
6. CONCLUSIONS AND RECOMMENDATIONS	49
6.1. Conclusions	49
6.2. Recommendations	49
7. FURTHER STUDIES	51
8. REFERENCES	53
9. APPENDICES	57
Appendix 1: Pattern for head distribution (hbg_level)	57
Appendix 2: Pattern NRW	57

Appendix 3: Pattern 102 detached and Apartment Housing	57
Appendix 4: Pattern 103 industrial use	58
Appendix 5: Scenario 2, pump malfunction	58
Appendix 6: Scenario 3 pattern-Fire Emergency	58
Appendix 7: Pathogen Intrusion pattern during pump malfunction	58
Appendix 8: Pathogen Intrusion pattern during pump Emergency fire	59

## List of Tables

Table 2.1: Summary of QMRA done for WDNs (Viñas et al., 2019). .....	6
Table 2.2: “Pipe Headloss Formulas for Full Flow (for headloss in feet and flow rate in cfs)” .....	14
Table 3.1: Summary of concentrations in untreated wastewater for the indicators/pathogens in the analysis used to calculate the ratios E.coli/pathogen. ....	34
Table 3.2: Calculated ratio between E. coli and the pathogen (Ec/Pathogen) in wastewater and that is used for estimating concentrations of pathogens in soil water. ....	34
Table 3.3: Calculated pathogen concentration in soil water using ratios between Ec/pathogen based on literature data in wastewater. ....	35
Table 4.1: Demand satisfaction ratios for Scenarios 1, 2, and 3.....	39
Table 4.2: Distribution of nodes with negative pressure using the PDA model.....	41
Table 4.3: Resulting intrusion rate, $Q_{int}$ , into EPANET used to calculate the intrusion mass flow of pathogens.....	41
Table 4.4: Calculated intrusion mass flow set into EPANET as a mass booster. It is calculated by multiplying the intrusion rate and calculated concentrations of pathogens. ....	41
Table 4.5: Modelled concentrations of pathogens (No/L) Campylobacter, Cryptosporidium, and Norovirus at 19:00 generated from EPANET.....	43
Table 4.6: Hourly probability of infection for scenario 2 and 3 presented for 5 <sup>th</sup> , 25 <sup>th</sup> , 50 <sup>th</sup> , 75 <sup>th</sup> , and 95 <sup>th</sup> percentile for each reference pathogen.....	44

## List of Figures

Figure 2.1: Flowchart QMRA derived from WHO Guidelines (WHO, 2016). .....	20
Figure 2.2: Flowchart describing how pathway links to exposure dose derived from WHO Guidelines (WHO, 2016). .....	22
Figure 3.1: Modeling process. ....	30
Figure 3.2: Hydraulic parameters used in EPANET 2.2 (a) general parameters applicable for DDA & PDA (b) PDA model (c) DDA model. ....	31
Figure 3.3: Head Pattern for low pressure conditions due to pump failure. ....	32
Figure 3.4: Definition of pressure due to groundwater that is included in determining the $\Delta H_{\text{pressure drop}}$ . ....	33
Figure 3.5: Hydraulic water quality modeling parameters used in EPANET 2.2 (a) Time, (b.) Quality, (c) Reactions. ....	35
Figure 3.6: Flowchart of the exposure assessment to get the exposure to be able to do the risk characterization. It includes hazard identification, chosen reference pathogens, barriers, and exposure pathways. ....	37
Figure 4.1: Statistical pressure distribution, minimum, median (50 <sup>th</sup> percentile), mean, maximum, 25 <sup>th</sup> percentile, and 75 <sup>th</sup> percentile during off-peak (00:00) and peak hour (13:00) for scenario1. ....	38
Figure 4.2: Pressure distribution for scenario 1 during off-peak demand for (a) 00:00 DDA and (b)00:00 PDA and during peak demand (c) 13:00 DDA and (d) 13:00 PDA. ....	39
Figure 4.3: Statistical pressure distribution, minimum, median (50 <sup>th</sup> percentile), mean, maximum, 25 <sup>th</sup> percentile, and 75 <sup>th</sup> percentile during peak hour times for scenario1-3. ....	40
Figure 4.4: Spatial distribution of low/negative pressure for scenario 2 at 13:00 for (a) DDA (b) PDA and scenario 3 at 19:00 for (c) DDA & (d) PDA. ....	40
Figure 4.5: Spatial distribution of pathogens (PDA)at 19:00. for Campylobacter (a) scenario 2, (b) scenario 3; Cryptosporidium (c) scenario 2, (d) scenario 3; and Norovirus (e) scenario 2, (f) scenario 3. ....	42
Figure 4.6: Statistical distribution of Campylobacter concentrations at 19:00 – 22:00 for scenarios 2 and 3. ....	42
Figure 4.7: Statistical distribution of Cryptosporidium concentrations at 19:00 – 22:00 for scenarios 2 and 3. ....	43
Figure 4.8: Statistical distribution of Norovirus concentrations at 19:00 – 22:00 for scenarios 2 and 3. ....	43



## 1. Introduction

The United Nation's (UN) sustainable development goal six, "clean water and sanitation", focuses on providing safe water for drinking and better sanitation services. Still, around 800 million people across the world lack access to affordable and safe drinking water today (WHO, 2020). According to "World Health Organization (WHO)", safe water is defined as "Safe drinking water that does not represent any significant risk to health over a lifetime of consumption, including different sensitivities that may occur between life stages" (WHO, 2017).

One frequently occurring health effect of unsafe drinking water is gastrointestinal illnesses (GII) that is caused by the poor quality of the drinking water containing bacteria, viruses, and protozoans. Säve-Söderbergh (2017) reported that up to 37 % of GII cases from drinking water was caused by the intrusion of contaminants into the water distribution network (WDN) (Säve-Söderbergh et al., 2017).

WHO (2017) lists examples of several pathogens that cause GII by consuming drinking water such as the bacteria *Campylobacter*, pathogenic *E. coli*, and *Salmonella*, the viruses *Norovirus* and *Rotavirus*, and the protozoans *Cryptosporidium* and *Giardia*. *Cryptosporidium*, for instance, is believed to be the major cause of GII cases in human beings across the world (Bjelkmar et al., 2017).

Water may also contain other microbes, that are not subject to this study, that pose a health risk through inhalation, like *Legionella*, or skin contact or wounds, like *Mycobacterium* that can cause tuberculosis (WHO, 2017).

Historically contaminated drinking water has caused numerous outbreaks of illness in the population. One famous example is the 1854 cholera outbreak in London where it was concluded that contaminated water drawn from specific pumps caused massive epidemics. This was demonstrated through statistical analysis and preventive actions where the pump handle was removed and microorganisms were identified or a theory for microbial infections was established (Paneth et al., 1998).

In modern times there are still several occasions of drinking water-induced GIIs reported globally. A well-known major outbreak occurred in 1993 in Milwaukee (Wisconsin), which was caused by *Cryptosporidium* and affected 30 % of the population (400 000 people). This happened due to the sub-optimal functioning of the barriers (filtration) in the drinking water treatment plant (DWTP) and could not manage to remove oocysts (Ballester & Sunyer, 2000; Bjelkmar et al., 2017).

The largest outbreak in Sweden happened in 2011 in Östersund, where about 27 000 people also were infected by *Cryptosporidium*. Several potential causes for the contamination were identified. It was concluded that the raw water contained higher levels of *Cryptosporidium* in the form of oocysts (in the contagious stage) than expected and that the WTP was not capable of treating that. It was also concluded that there was an overflow in the wastewater treatment plant (WWTP) which contributed to the increased levels of oocysts in the raw water and that there was incorrect piping so that wastewater was discharged into streams that lead to the raw water source. The actual source for the outbreak was however not conclusively identified. There are speculations that the increasing average temperature may promote the spreading of *Cryptosporidium* (Schönning et al., 2011).

## 1.1. Background

Significant cases of GII have been attributed to the contamination in WDNs and the proportion of these cases is observed to be on the rise (Blokker et al., 2014). Säve-Söderbergh (2017) estimates 37% of total GII cases to have originated from WDNs globally. In the “United States of America (USA)”, WDN intrusions were linked to 30% of GII cases and there has been a tremendous increase in proportion since 1991 while in Europe, 31% of GII was observed in 61 outbreak studies conducted (Blokker et al., 2018).

WDNs are critical infrastructure within every settlement from small villages to towns and major cities (Wéber et al., 2020). The WDN consists of water source(s), pipelines, and hydraulic components such as pumps, tanks, and valves interconnected to deliver recommended quality and quantity of water at recommended pressure (Mandel et al., 2015; Ostfeld et al., 2004). Different loading conditions can be expected in a WDN for instance, demands at the nodes (connection points), emergency fire demands, peak demands, and critical demands due to malfunctioning of one or more of the system components (Mandel et al., 2015; Ostfeld et al., 2004).

Since the WDN is the last point before the water reaches the consumer it is important to have proper functioning of the WDN to maintain the gains made in the water supply chain and to assure public health (Islam et al., 2017; Wéber et al., 2020). According to Viñas et al (2019), the WDN acts as the last physical barrier that guards against infringement before the final consumer. Being at the end of the WDN, there is a low probability of detecting and remediating a contamination event in time before water consumption hence the need for maintaining the WDN’s integrity.

The expansion of WDNs to meet the growing water demand and aging among other reasons have hampered the maintenance of WDN’s integrity (physical, hydraulic, and quality) between the water consumers and the treatment plants (Nyende-Byakika et al., 2013; Simões & Dong, 2018; Teunis et al., 2010). The ability of a WDN to protect internal drinking water from external contamination is referred to as physical integrity (Besner et al., 2011).

The associated water contamination pathways include pipe breaks, cracks, uncovered tanks/reservoirs, faulty or incorrect pipe connections (including crossflow connection and backflow devices) may result in intrusion of contaminants into the WDN (Besner et al., 2011; Viñas et al., 2019). Hydraulic integrity, on the other hand, refers to the ability to retain adequate water pressure, age, and flow in a WDN considering nodal and fire demands (Besner et al., 2011). Internal processes (quality) are direct chemical and (micro)biological reactions that may occur due to pipe material, treatment processes, and raw water quality variations (Davis et al., 2014).

The failure to maintain the adequate pressure gradient, in the presence of pipe breaks, cracks, and/or holes, is the main driver for intrusions into WDNs (Besner et al., 2011; Davis et al., 2014). Intrusions can in turn negatively impact water quality due to the presence of pathogens in soil water within the drinking water pipe surroundings and from cross-flow connections (Yang et al., 2016). WDN’s with irregular water supply are highly vulnerable to intrusion contamination as they are characterized by low water pressures for long durations lasting from hours to days as well as reduced physical integrity such as high leakage, inadequate disinfectant residuals, cross-flow connections, and non-standardized connections to water main pipeline. Such WDN’s are mostly reported in developing

regions and high contamination risks are prevalent as seen from various disease outbreaks and rising GII cases (Besner et al., 2011).

Intermittent supply is rare in developed countries however negative pressure conditions still occur and take the form of transients as well as sustained events. Transient events occur due to pumps shutting down suddenly and can have durations ranging from seconds to minutes. Sustained low pressure conditions can occur as a result of main pipeline breaks (causing free-low), planned repairs from unexpected extreme weather, and failure events (Besner et al., 2011). An example is a power blackout in the Northeast USA of 14<sup>th</sup> August 2003, that affected approximately 50 million consumers resulting in boil water advisory (Besner et al., 2011).

Various incidences of waterborne disease outbreaks and subsequent GII resulting from compromised WDN have been observed across the world (Viñas et al., 2019). In Finland in 2007, Nokia area, 6500 people got ill because wastewater containing pathogens was fed into the drinking water through a crossflow connection (Viñas et al., 2019).

In Sweden between 1980 and 2007, 27 cases of waterborne outbreaks associated with WDN were reported. This accounted for 34% of the total outbreaks in the period (Viñas et al., 2019). According to Mena et al (2008), the “*Centre for Disease Control and Prevention*”, in the USA, reported 57 outbreaks of waterborne diseases associated with backflow intrusion in WDN from 1981 to 1998. Recently in the USA, the ratio of WDN intrusion to other contaminant sources in the drinking water is estimated to be 1:1 (McInnis, 2004). Payment et al (1991, 1997, 2000) as cited by McInnis (2004) suggest that out of the 99 million GII cases observed in the USA, a third are associated with microbes in the WDN.

## **1.2. Aim**

This study aimed at simulation of the impacts of prolonged negative or low pressure conditions on hydraulic characteristics as well as water quality parameters in a water distribution network. It sought to identify critically affected areas of the water distribution network for potential quality monitoring with sensors, and quantify the associated health impacts.

## **1.3. Specific objectives**

- Using hydraulic simulation, predict peak negative pressures in a WDN under sustained low-pressure conditions and determine areas critically affected by the negative/low pressures.
- Estimate pathogen intrusion quantities into the WDN under sustained low pressure conditions.
- Using extended period hydraulic and water quality modeling, determine the transportation and fate of pathogens in the WDN and obtain pathogen concentration (dose) at critical times.
- Determine the health risks due to pathogen intrusion in WDN using QMRA.
- Using the identified critical low pressure areas and health risks, propose an early warning system for quality monitoring such as a system of sensors.

#### **1.4. Limitations**

- The simulation focused only on continuous sustained low pressure in the system with constant intrusion rates of pathogens in the WDN, however, intermittent intrusions are possible in real-life cases and the concentration of pathogens in the soil water may not be constant. This could have been the source of high estimates for pathogen intrusions resulting in higher risk estimations.
- Reactions in a water distribution system were not considered, for instance, inactivation of pathogens by disinfectants and interaction of pathogens with biofilm. This could have resulted in the overestimation of pathogens at the nodes.
- Water sampling and testing along the distribution pipelines to determine the concentration of pathogens were not done, hence the study relied on information from literature sources for sampling done close to the nearby areas increasing the chances of overestimation or underestimation.

## 2. Hydraulic Modeling and QMRA

Various models have been developed that can estimate potential health risks due to pathogen intrusion in WDNs. Pathogen rates of intrusion into the network can be adequately described using developed hydraulic models. With the hydraulic models, it is possible to model intrusion and transportation of pathogens into the WDN (Viñas et al., 2019). EPANET model is such an example that can be used for hydraulic simulation as well as modeling water quality in WDN after the intrusion of pathogens (Rossman et al., 2020). MIKE URBAN+ is one other application built on EPANET and has additional water distribution tools that can simulate intrusion as well as transport in WDN (DHI Water & Environmental, 2011). EPANET MSX on the other hand is an EPANET extension with the capacity to model how multiple water quality species interact within the WDN, for instance, interactions among pathogens and the residual chemical disinfectants and pathogens and biofilms (Hatam et al., 2018). Other models include Water network management (Aquis), which is an advanced tool with the capability for hydraulic simulation, thermal analysis, operational optimization & planning, and water quality tracking (CTI resources, 2021; Larsen et al., 2017; Schneider Electric, 2021).

Different approaches can be used for the assessment of risk including identification and estimation of the risk levels in WDNs. The most common approaches include qualitative, quantitative, and semi-quantitative methods (Pettersson & Ashbolt, 2016). Qualitative methods, for instance, sanitation surveys, are less resource-intensive and easy to use and reasonable estimation of risks can be obtained. Semiquantitative methods, such as more complex risk matrixes, will provide an in-depth assessment of WDN's hazards. Quantitative methods on the other hand can explicitly provide quantification of health risks in terms of annual infection risks (Viñas et al., 2019).

According to Viñas et al (2019), Quantitative Microbial Risks Assessment (QMRA) is the commonly used framework for the estimation of the health impacts associated with pathogens intrusion risks. QMRA is useful for estimating potential infection risks due to pathogen contamination events in WDNs. Expected illness cases, as well as the maximum possible limit of illness cases, can be determined. Similarly, statistical intervals such as the upper confidence limit can be established (Viñas et al., 2019). The effectiveness of QMRA can be increased by combining with other models for instance hydraulic models, capable of simulating pressure drops in WDN networks, and water quality models, that are capable of simulating the behavior of various quality species within the WDNs (Viñas et al., 2019). Several studies have used these models in different countries and for various intrusion cases as highlighted in Section 2.1.

### 2.1. Applications of hydraulic modeling and QMRA

This section describes several applications of hydraulic modeling coupled with QMRA. Viñas et al (2019) summarized some of the various incidences across the world where QMRA models coupled with hydraulic models were used in WDNs as can be seen in Table 2.1. and further described in Sections 2.1.1 to 2.1.5.

Table 2.1: Summary of QMRA done for WDNs (Viñas et al., 2019).

Study	Network site	Risk event	Pathogen	Methodology
(Blokker et al., 2018)	Netherlands	Main repair	<i>Giardia</i> , <i>Campylobacter</i> , <i>Cryptosporidium</i> , <i>Enterovirus</i>	QMRA coupled with hydraulic modelling. Used EPANET to simulate the transport of contaminated water. SIMDEUM for consumption patterns, and Monte Carlo simulations for risk characterization.
(Storey et al., 2004)	Sweden	Biofilm	<i>Legionella</i>	QMRA modeling. Detachment of <i>Legionella</i> was determined experimentally, as well as disinfection data. Monte Carlo simulations were used for risk characterization.
(McInnis, 2004)	City in North America	Intrusion	<i>Giardia</i> , <i>Fecal streptococci</i>	QMRA coupled with hydraulic modelling.
(Van Liverloo et al., 2007)	Netherlands	Multiple contamination events	<i>Giardia</i> , <i>Campylobacter</i> , <i>Cryptosporidium</i> , <i>Enterovirus</i>	QMRA coupled with hydraulic modelling.
(Teunis et al., 2010)	United States	Intrusion	<i>Rotavirus</i> , <i>Norovirus</i>	QMRA coupled with hydraulic modelling. Used commercial software to do surge modeling. EPANET-MSX for water quality modeling coupled with Monte Carlo simulations for risk characterization.
(J. Yang et al., 2011)	United States	Main repair	<i>Norovirus</i> , <i>E. coli O157</i> , <i>Cryptosporidium</i>	QMRA coupled with hydraulic modelling. Simplified model from Teunis et. al. (2010b)
(Mena et. al., 2008)	United States	Cross-connection	<i>Salmonella</i>	QMRA coupled with hydraulic modelling. Used a distribution network simulator to estimate transport of contaminated water and Monte Carlo simulations for risk characterization.

### 2.1.1. Main pipeline repair

This section describes three different studies involving the repair of WDN main supply pipes where hydraulic modeling and QMRA were applied. The studies were done in different cities at different periods.

#### Netherlands, Blokker et al., 2018

In Netherlands, QMRA along with hydraulic models were used to estimate the health impacts of bacteria *Giardia* and *Campylobacter*, *Cryptosporidium oocysts*, and *Enterovirus* after the main repair event (Blokker et al., 2018). A WDN in part of Zandvoort town was used, which served nearly 1000 households, 3 hotels as well as 3 beach clubs. The QMRA-hydraulic modeling followed the following steps: First was specifying the contamination event (after repair of WDN). The second step involved hydraulic modeling with EPANET where flow and spreading of the contaminants were determined. In the third

step, the consumption step, the demand patterns were simulated using “SIMulation of water Demand, and End-Use Model (SIMUDEM)”. The model can predict demand patterns by combining predicted human behavior, water consumption statics, and technical specification (Blokker et al., 2017). The volume of water consumed and the concentration of pathogens was used to determine ingestion in the fourth step. Dose-response models were used to determine infected people as a result of water ingestion in the infection (fifth) step. Finally, in the event risk, the infection risks per event were determined. Monte-Carlo simulation was used for sensitivity analysis of various dose ingestion factors (Blokker et al., 2018).

The results, of sensitivity analysis, suggested that the most critical parameter that influenced the dose ingested (contaminants consumed) was the concentration of contaminants while the dose-response model adopted had a high influence on the infection risk. Blokker et al (2018) indicate over-estimation of risks is possible in standard QMRA when diurnal patterns of consumption are neglected. From sensitivity analysis, consumption volume was found to have less influence on the impacts. It was recommended that issuing a boiling advisory and opening of one valve before opening the isolated repair section was a more effective mitigation measure. It could reduce 50 to 80 % of infection risks. Better sampling time was also proposed for the first 4 hours after repair in which the detection probability for indicator pathogen *E.coli* was found to exceed 80% for the optimal location sampling. However Dutch regulation for indicator organism (*E.coli*/100ml) sampling after the repair was a day after the repair event and this yielded a 25 % probability of detection due to flushing of the contaminant in the consumers' toilets, kitchen taps, and showers (Blokker et al., 2018).

### **The USA, Yang et al., 2011**

Using a transient-based hydraulic model developed by Teunis et al (2010) in the USA, Yang et al (2011) Investigated various conditions that influenced the infection risks from *Norovirus* and proposed potential mitigation measures for risk reduction. For exposure data, he evaluated intrusion characteristics as well as the fate of *Norovirus* transportation in WDN. The factors considered included concentration of virus close to the WDN, chemical disinfectant residual present, leakage orifice sizes, duration of low pressure event, and the number of low pressure nodes (Yang et al., 2011). The results indicated the low pressure event duration as the most sensitive factor hence pressure transient management was necessary to reduce the severity of these events. It was further recommended a 0.2 mg/L chlorine residual be maintained to act as a disinfectant in case of low pressure intrusions (Yang et al., 2011). In vulnerable sections, leak repair and detection were necessary as well as close monitoring for cross-flow intrusion cases (Yang et al., 2011).

### **The USA, Yang et al., 2015**

In the USA during the main repair of the WDN, Yang et al (2015) simplified the model applied by Teunis et al (2010) for estimating the impacts of *Norovirus*, *E.coli*, and *Cryptosporidium*. The model provided for estimation of risks for first consumers on the WDN downstream of the repaired break area. Flushing of the pipe was deemed effective and hence eliminated the need for modeling contaminants transport and mixing along the pipeline. Impacts of flushing and various disinfection criteria were investigated in relation to their effectiveness in mitigating health impacts of intrusion after the main repair (Yang et al., 2015). The risk model was simple but similar to the previous models and was implemented in seven different steps. The steps involved determining the pathogen levels

around the WDN main pipeline, estimating the concentrations within the main pipeline in the second step then evaluating pathogen reduction levels due to flushing. Consumer consumption volume was then estimated followed by the determination of pathogen infection dose-response levels. “*Monte-Carlo simulation*” was applied for risk sensitivity analysis and finally, risk management and mitigation options were evaluated (Yang et al., 2015). When no flushing and disinfection was used, high infection risk levels, exceeding the recommended annual levels of 1 in every 10,000 people, was observed for all the pathogens investigated (Yang et al., 2015). *Norovirus* was found to have a high infection risk during low pressure conditions compared to other pathogens. Flushing in combination with chemical disinfection was found to reduce the infection risk from viruses by a 7-log scale thus achieving the recommended target (Yang et al., 2015).

### **2.1.2. Biofilm**

#### **Sweden, Storey et. al, 2004**

In Sweden, hydraulic modeling and QMRA were used to estimate the health impact of *Legionella* in the WDN under normal conditions as well as in the presence of biofilms and thermophilic amoeba (Storey et al., 2004). The QMRA was developed assuming maximum risk (maximum risk curve,  $r=1$ ) for the pathogen *Legionella* in WDN. The results were compared to the conventional treatment methods for *Legionella*. Hydraulic simulation of biofilm detachment events was done for both laminar and turbulent flow conditions and the results were taken for estimation of risks in QMRA. Samples for chemical and thermal treatment were also taken at appropriate steps for all the scenarios. The results indicated a high influence of both biofilms and thermophilic amoeba with an increase in resistance to regular thermal treatment by log scales of 1 and 2 for biofilms and thermophilic amoeba respectively. The risk levels exceeded the United States Environmental protection Agency (USEPA) guideline of  $10^{-4}$  in most of the tested incidences (Storey et al., 2004). The exceedance was partly due to the sensitivity of the risk model used and due to a lack of credible dose-response information for *Legionella*. The modeling of the interaction between legionella and the biofilm and *Legionella* and amoeba was achieved in which biofilm was found to increase legionella infection risks (Storey et al., 2004).

### **2.1.3. Intrusion**

Two cases of intrusion from North America and the United States were described in this section.

#### **North America, McInnis, 2004**

McInnis (2004) used hydraulic modeling and QMRA in a city in North America to estimate the impact of bacteria *Giardia* and fecal *Streptococci*. The network served approximately 100,000 consumers and consisted of a 1350mm diameter: 5,500m long main pipeline from the pumping station. The WDN was served by 2 pumps with flows of 313 l/s and 740 l/s located in different areas within the WDN (McInnis, 2004). The hydraulic simulation was done using EPANET and by shutting the bigger pump to create transient conditions. For every node that experienced a drop in nodal pressure, intrusions were determined by the transient model. Total nodal intrusions were considered mass sources in the EPANET quality model and the distributions around the system were modeled to find the dose at the consumer taps. QMRA was used for modeling the potential health risks of the intrusion into the WDN. From the study, it was noted that transient conditions can trigger

unacceptable amounts of pathogen intrusion into the WDN leading to high risks of infection. It was noted that the hydraulic parameters were only suitable for the assessment of possibilities of intrusion as well as the distribution of intrusions in the system but were not suitable for risk reduction. It was thus recommended that a risk-based approach is necessary for estimating the effects and thus propose mitigation measures (McInnis, 2004).

### **The USA, Teunis et al., 2010**

The health effects of the intrusion of *Norovirus* and *Rotavirus* in the WDN due to contamination events from sewage were studied in detail in the USA (Teunis et al., 2010). The WDN was composed of 1128 nodes, junctions, with a total of 269 km (167) miles of piping comprising 1369 pipes. The diameters of the pipe, links, ranged from 600 mm to 3000 mm. Supply was from four wells with five pumping stations and two elevated storage reservoirs. The system served 33,000 consumers with annual mean and maximum daily demands of 22.7 and 50.3 thousand cubic meters respectively.

QMRA with hydraulic modeling and Monte-Carlo simulation were used. Hydraulic modeling of the surge was done with commercial modeling programs, such as InfoSurge while EPANET-MSX was used for modeling water quality parameters. The concentration of virus in sewage was obtained from existing literature and worst-case scenarios were used in the modeling exercise. Virus intrusion into the WDN was determined based on negative pressure events in the system. Intrusion viral numbers were influenced by concentration in soil media, leakage size, and the time taken by the negative pressure event (Teunis et al., 2010). A power outage on one of the pump stations was used to simulate the pressure surge because of taking one pump offline. Vulnerable virus intrusion nodes were predicted to be 118 and the transportation of the contaminants into the WDN was modeled with EPANET. To simulate transport behavior of the pathogens (decay) as well as interaction with disinfectants (inactivation); multi-species EPANET-MSX was employed to give more accurate numbers the consumers were exposed to at various nodes basing on initial nodal intrusions. Exposures and infection by consumers were based on nodal population, the actual amount ingested, the likelihood of ingestion coinciding with virus contamination peak at the node, and the lethality of the virus under observation.

The results indicated dependency of risks on water ingestion coinciding with the viral peak in the affected node. The duration of Pressure drop events was identified as the main contributing factor to infection risks. It determined how long the virus stayed in the WDN as well as the likelihood of the virus pathogens' peak at the demand node. It was observed the risk of infection was a hundred times higher for a thousand second event compared to a one-second event. The concentration of the virus in sewage depicted minimal impact on the resulting average observed risk of infection with a notable 6-log concentration increase only increasing the infection risk by a 1-log scale (Teunis et al., 2010).

#### **2.1.4. Multiple contamination events**

##### **Netherlands, van Liverloo et al., 2007**

According to van Liverloo et al (2007), QMRA with hydraulic modeling was used to estimate consumer infection risk resulting from fecal contamination of WDNs in various parts of the Netherlands. Effects of “*Giardia*, *Campylobacter*, *Cryptosporidium* and *Enterovirus*” originating from various sources were investigated. Concentration data for “*thermotolerant coliforms (E.coli)*” were derived from an outbreak incidence and 49

additional non-outbreak cases recorded in Dutch WDNs without chlorination from 1994 to 2003 (van Lieverloo et al., 2007). The mean daily ingestion volume of 0.177 l/person was used and it represented an average value in the Netherlands according to van Lieverloo et al (2007). The probability of infections was determined based on infection risk considered (risk per event or the annual risk due to several contamination events). The outcome of the studies indicated higher risks associated with *Campylobacter* as well as *Enterovirus* though high uncertainties were also observed. Considerably high variabilities were noted for pathogens to the coliform ratio found in environmental samples hence limiting the approach adopted for the study for futures applications. High ratios of *Enterovirus* to coliforms were attributed to soil and groundwater, which are the highly probable sources of fecal contamination detected in WDNs. Van Lieverloo et al (2007) suggested the use of epidemiological assessments and efficient tracking as well as characterizing contamination sources for estimating actual risks.

### **2.1.5. Crossflow connection**

#### **The USA, Mena et al., 2008**

QMRA was used for the prediction of impacts of intrusion of pathogen *Salmonella* in the WDN as a result of cross-flow connection involving wastewater (Mena et al., 2008). The expected number of salmonella infection were determined as well as corresponding illness cases due to water ingestion. Using USEPA's distribution system simulator (DSS), a lab-scale experiment was conducted simulating a cross-flow connection. The data was compared to the areal cross-flow connection incidence experienced in Pineville, Louisiana in the United States in May 2000 (Mena et al., 2008). Sixty households were impacted by the incident, which occurred when a pump from a sewage utility was accidentally connected to WDN during a routine repair (Mena et al., 2008).

The DSS was made of 16 separate loops comprising 152.4 mm diameter iron pipes. The loop had been in operation for a long time and could simulate biofilm and corrosion conditions of the pipe walls just like in the real WDN. Approximately 835 liters of feed water were circulated in a 25 m independent loop. The flow rate in the loop was 36 l/h and the retention time was  $24 \pm 2$  hrs. just before discharge. The normal scenario was simulated with feed water (tap water) for 4 weeks after which 8.35 liters per day of wastewater was injected for the 90 day study period (Gibbs et al., 2003). The study adopted different exposure scenarios and the probability of infection, as well as the probability of illness for each scenario, were determined.

The exposure represented varying concentrations of salmonella as well varied rates of attack for waterborne *Salmonella* (Mena et al., 2008). For the lowest concentration of salmonella, the infection risks ranged from 10 %, for a single-day exposure, to 1-log increased risk for other higher concentration scenarios. A 99 % infection risk was observed after 30 and 90 day exposure periods (Mena et al., 2008).

From the previous studies, it can be demonstrated that “*hydraulic and water quality modeling*” is necessary for determining the distribution of various pathogens in the WDN as well as the various relation occurring within the pipes and hence useful for determining the dose at a particular point in the WDN. Hydraulic modeling cannot however in itself estimate the risks posed to humans as a result of consumption of contaminated water (McInnis, 2004). This then necessitates the use of a risk modeling program that can estimate annual risks and hence making it possible to determine several risk management

and mitigation options (Yang et al., 2015). The next section describes various tools that have been applied, by various researchers and for this case study, in estimating the health impacts of pathogen intrusion in a WDN. The basic operational principles and capabilities of the hydraulic, water quality and risk modeling tools are discussed.

## **2.2. Hydraulic and QMRA modeling tools**

This section describes the tools that can be used for hydraulic simulation and QMRA. This includes Mike Urban+ and EPANET 2.2, built based on an EPANET engine and suitable for hydraulic analysis. Water network management (Aquis), which is an advanced tool with the capability for hydraulic simulation, thermal analysis, operational optimization & planning, and water quality tracking (CTI resources, 2021; Larsen et al., 2017; Schneider Electric, 2021). The others are EPANET MSX which is capable of multi-species water quality analysis, and the QMRA tool used for risk analysis.

### **2.2.1. Mike Urban+**

MIKE URBAN+ is an advanced modeling tool for water distribution available on the market (DHI Water & Environmental, 2011). MIKE URBAN+ WD (water distribution) is capable of analysis involving the entire WDN or part of it under various hydraulic conditions such as steady-state analysis, extended period simulation, and analysis due to water hammer situations. Water quality analysis can be incorporated in any of the conditions when necessary. It utilizes the publicly available EPANET engine and Water Distribution (WD) tools/engine, a product of the Danish Hydraulic Institute-DHI, for modeling WDNs. With the EPANET engine, WDN pipe flow and water quality analysis can be accomplished. The WD tools have the capability for water hammer analysis, calibration of the roughness of pipes, analysis involving fire flow, simulation of variable speed-drive pumping units, and extended controls adopting a modified EPANET. WD asset data can also be analyzed using the WD tools (DHI Water & Environmental, 2011).

In Mike Urban+, a new water distribution model (WDM) can be developed by direct entry of data as well as importing geodata from GIS-based databases or existing models. Maps of the models can as well be imported and used as background hence making it necessary to place junctions and pipes with accuracy in respect to the site conditions (DHI Water & Environmental, 2011). Different features of MIKE+ WD are described below.

#### **Flow in pipes**

EPANET engine is used in MIKE URBAN+ to compute flow, pressure, and quality of water in WDNs under steady or quasi-steady-state conditions. EPANET uses a universal Global gradient algorithm to solve a network of nodes (junctions) and links (connecting pipes) equations (Rossman et al., 2020). The algorithms solve a system with sparse, symmetrical, and positively-definite linear equations for every iteration. This enables a highly sparse matrix, which is efficient, techniques to be applied to obtain the relevant solution. Flow continuity is maintained by the algorithm at all nodes after the first iteration during the second step. Lastly, the algorithm can manage pumps and all valves within the system with no change to the equation matrix structure when there is a change in the status of the components. Key features of pipe flow in MIKE URBAN+ include steady-state and extended-period simulations as well as rule-based simulation (DHI Water & Environmental, 2011). Detailed features of EPANET and governing equations will be discussed in Section 2.2.2.

## **Water Quality**

EPANET water quality solver uses the Lagrangian method, which is the most efficient time-driven method. Key parameters computed in the analysis of water quality include water age in the WDN, source tracking, determination of dissolved substance's fate, and determination of substance's growth or decay. Mass inflow rates and substance concentrations are used to define the quality of the water sources. Modeling of bulk flow is achieved with n:th order kinetics while wall reactions are modeled with zero or first-order kinetics. Decay or growth of water quality parameters can be modeled up to allowable limits while reaction coefficients for pipe walls can be correlated to roughness coefficients of pipes. In MIKE URBAN+, water age, chlorine concentration, and path & pollutants concentration analyses are the key quality aspects modeled (DHI Water & Environmental, 2011).

## **Water Distribution Tools**

MIKE URBAN+ provides extra tools than the normal EPANET can provide, for various functions in the simulation of WDN hence more realistic conditions can be simulated. Some of these tools include the Fire Flow tool, which lets you evaluate the possible flow considering a given design pressure or residual pressure considering a given design flow (DHI Water & Environmental, 2011).

The roughness calibration tool for pipes automatically modifies roughness coefficients to match observed field pressure to best indicate actual system occurrences. Hazen-Williams, Chezy-Manning, and Darcy-Weisbach friction loss formulae can be applied for determining the roughness coefficients for pipes (DHI Water & Environmental, 2011).

Proportional Integral Differential (PID) tools allow controlling the simulations for WDN in real-time. Description of various controllable components is possible in PID as well as defining complex operation logic for regulators which are interdependent. All types of valves and pumps can be specified (DHI Water & Environmental, 2011).

Variable Speed-Drive (VSD) Tool is suitable for automatically controlling node pressure to maintain required levels by adjusting a VSD pump rotational speeds (DHI Water & Environmental, 2011).

Extended Rule-Based tools or Controls gives the flexibility to model multiple conditions existing in the system over extended periods of simulation to control link settings and status. Multiple pump chains and valves can be modeled with this tool (DHI Water & Environmental, 2011).

Pressure driven Analysis tool is available and in this tool, Wagner equation is applied to solve for demands at nodes based on available pressure rather than the traditional demand-driven method where a constant demand, defined before simulation and independent of nodal pressure, is used (DHI Water & Environmental, 2011).

Pressure Zone Mapping tool aids visual of hydraulic interconnectivity of different WDN parts and indicates where the hydraulic grade line (HGL) breaks (DHI Water & Environmental, 2011).

The water hammer tool is useful for the simulation of unsteady flow in pressurized systems transporting liquids. This tool uses finite-difference to solves continuity equation as well

momentum equation and it is thus based on high order schemes of implicit nature. In water hammers, pump start and trip-off, pumping station protection, and power failure can be modeled (DHI Water & Environmental, 2011).

### 2.2.2. EPANET 2.2

Based on EPANET 2 engine, this version has additional capacity for hydraulic analysis involving pressure-dependent demands. Similarly, tank overflows can as well be simulated. Different components are discussed in this section.

#### Demand-driven model

This model assumes a fixed demand that must always be met in the distribution system. This can sometimes lead to negative pressure at some nodes (Rossman et al., 2020)

Considering a WDN with “*N nodes and NF fixed nodes*”, such as reservoirs and storage tanks, with a flow  $q_{ij}$  in links (pipes) joining nodes  $i$  to  $j$ . Flow from  $i$  to  $j$  is considered positive while from  $j$  to  $i$  is considered negative. The flow-friction losses relationship within pipes is expressed as in Equation 1 (Rossman et al., 2020).

$$h_{Lij} = r q_{ij} |q_{ij}|^{n-1} + m q_{ij} |q_{ij}| \quad (1)$$

Where  $h_{Lij}$  = head loss,  
 $r$  = resistance coefficient,  
 $n$  = flow exponent  
 $m$  = minor loss coefficient

Different formulae (*Hazen-Williams, Darcy-Weisbach, and Chezy-Manning* ) are available for representing head loss and the value of  $r$  will depend on the formula used. Ignoring minor losses, Equation (1) can be simplified as (Sami, 2018)

$$h_L = A q^B$$

where  $h_L$  = friction headloss in pipes  
 $A$  = resistance coefficient  
 $q$  = flowrate (volume/time)  
 $B$  = flow exponent

The resistance coefficient and flow exponent for the 3 formulae can be obtained as per the expressions in Table 2.2 (Sami, 2018).

Table 2.2: “Pipe Headloss Formulas for Full Flow (for headloss in feet and flow rate in cfs)”

Formula	Resistance Coefficient (A)	Flow Exponent (B)
<i>Hazen-Williams</i>	$4.727 C^{-1.852} d^{-4.871} L$	1.852
<i>Darcy-Weisbach</i>	$0.0252 f(\epsilon, d, q) d^{-5} L$	2
<i>Chezy-Manning</i>	$4.66 n^2 d^{-5.33} L$	2

Where: C = Hazen-Williams roughness coefficient  
 $\epsilon$  = Darcy-Weisbach roughness coefficient (ft)  
f = friction factor (dependent on  $\epsilon$ , d and q)  
n = Manning roughness coefficient  
d = Pipe diameter (ft)  
L = Pipe length (ft)  
q = flow rate (cfs)

The head loss for a pump operating between nodes i and j is represented by the power-law Equation 2 (Rossman et al., 2020)

$$h_{Lij} = -w^2 (h_0 - r(q_{ij}/\omega))^n \quad (2)$$

Where:  $h_0$  = pump shutoff pressure (head), s  
w = pump relative speed,  
r and n = pump curve coefficient  
 $q_{ij}$  = should be positive

For Energy conservation across a pipe (link) connecting node i and node j,

$$h_i - h_j = h_{Lij}(q_{ij}) \quad (3)$$

Where:  $h_i$  and  $h_j$  = hydraulic heads at the respective nodes

From the principle of conservation of mass, total inflow and outflow at node i should be equal (Rossman et al., 2020).

$$\sum_j q_{ij} - D_i = 0 \quad (4)$$

Where: Summation is done across all nodes j linked to node i

$D_i$  = fixed demand required at node i

At fixed nodes (tanks and reservoirs) and for a known set of heads, the solution for head h at every node (junction) and flow q in every pipe (link) is sought which satisfies Equations 3 and 4 (Rossman et al., 2020)

EPANET uses a universal Global gradient algorithm (GGA), to solve a network of nodes (junctions) and links (connecting pipes) equations. GGA linearizes conservation equations using the Newton-Raphson iterative method. Nodal heads are first obtained by solving a (N x N) sparse system of symmetrical and positively definite linear equations. The new flow is computed in the second step by applying the scaler updating function to every link (Rossman et al., 2020).

Initial flow in every link is estimated by the GGA algorithm which may not satisfy the principle of flow continuity. New nodal pressure (heads) is then determined from a solution of the linear equation for  $h$  at every iteration.

$$Ah = F \quad (5)$$

Where:  $(A \times N) =$  square symmetric coefficient matrix

$h = (N \times 1)$  vector of unknown nodal heads

$F = (N \times 1)$  vector of right hand side terms

The matrix diagonal coefficient elements are:

$$A_{ii} = \sum_j \frac{1}{g_{ij}} \quad (6)$$

While off-diagonal elements are

$$A_{ij} = -\frac{1}{g_{ij}} \quad (7)$$

Where:  $g_{ij} =$  gradient of headloss in the links due to flow.

For pipes

$$g_{ij} = nr|q_{ij}|^{n-1} + \frac{\partial r}{\partial q_{ij}} |q_{ij}|^n + 2m|q_{ij}| \quad (8)$$

While for pumping units

$$g_{ij} = n\omega^2 r (q_{ij}/\omega)^{n-1} \quad (9)$$

$F_i$ , the term on the right-hand side, for every node  $i$ , consists of imbalanced flow and a factor for flow correction.

$$F_i = \sum_j (q_{ij} + h_{Lij}/g_{ij}) - D_i + \sum_f H_f/g_{if} \quad (10)$$

Where: The last term is applicable to links between node  $i$  and fixed node

After computation of new head from solving Equation 5, new flows in every link are computed using:

$$q_{ij} = q_{ij} - \Delta q_{ij} \quad (11)$$

Where

$$\Delta q_{ij} = (h_{Lij} - h_i + h_j) / g_{ij} \quad (12)$$

Flow continuity is maintained by the GGA algorithm at all nodes after the “*first iteration*” during the second step. Iterations continues until an acceptable convergence is achieved which may be based on negligible flow change or when the residual errors linked with conservation equations (mass and energy) are satisfied (Rossman et al., 2020).

## Pressure Driven Demand Model

Wagner equation is applied to solve for demands at nodes ( $qD_i$ ) based on available pressure ( $p_i$ ) rather than the traditional demand-driven method where a constant demand, defined before simulation and independent of nodal pressure (Rathi & Gupta, 2017). Pressure  $p_i$  is the hydraulic head ( $h_i$ ) and elevation ( $E_i$ ) difference. Pressure-based nodal flows are given by Equation 13 (Rossman et al., 2020).

$$qD_i = \begin{cases} D_i & p_i \geq P_f \\ D_i \left( \frac{p_i - P_0}{P_f - P_0} \right)^{\frac{1}{\epsilon}} & P_0 < p_i < P_f \\ 0 & p_i \leq P_0 \end{cases} \quad (13)$$

Where  $D_i =$  Normal demand at node  $i$  when  $p_i \geq P_f$

$P_0 =$  minimum pressure, below which demand is zero

$\frac{1}{\epsilon} =$  pressure function exponent (usually set to 0.5  
– flow through orifice

Head loss in an imaginary (virtual) link in relation to demand outflow through a node  $i$  to a fixed head ( $P_0 + E_i$ ) virtual reservoir can be represented by Wagner's inverted power function (Rossman et al., 2020).

$$h_i - P_0 - E_i = R_{D_i} qD_i^\epsilon \quad (14)$$

Where:  $R_{D_i} = (P_f - P_0) / D_i^\epsilon -$   
coefficient of resistance for the virtual link

GGA matrix system of equations can utilize the expression in which pressure-dependent demands are  $qD$  are modeled as unknown flows through the virtual links. Conforming to Wagner equation. The virtual links do not affect the size of the network nor the corresponding coefficient matrix  $A$ . Head loss and the respective gradient can then be evaluated across the virtual link basing on various conditions: when the actual demand  $qD$  exceeds the normal demand  $D$ ; when the actual demand  $qD$  is below zero and during normal demand.

Incorporating head loss and gradient functions in the GGA matrix yields the following matrix functions.

Diagonal elements of matrix  $A$  representing node  $i$

$$A_{ii} = A_{ii} + 1/g_{Di} \quad (15)$$

Factor  $F$  representing node  $i$

$$F_i = F_i + D_i - q_{Di} + (h_{LDi} + E_i + P_0)/(g_{Di}) \quad (16)$$

*“Note:  $D_i$  is added to  $F_i$  to cancel out having subtracted it from the original  $F_i$  value appearing in Eq 10”.*

Demand at the nodes  $i$  is updated once the new set of heads at the nodes has been computed by subtracting flow change (Rossman et al., 2020).

$$\Delta q_{Di} = (h_{LDi} - h_i + E_i + P_0) / (g_{Di}) \quad (17)$$

The linear equation is solved using the Cholesky method while initial flows  $q_D$  are set to normal demand  $D$  and flow through the emitter is set to zero.

Lastly, the algorithm can manage pumps and all valves within the system with no change to the equation matrix structure when there is a change in the status of the components. Others include Steady-state and extended-period simulations, as well as rule-based simulation, which can be implemented with EPANET.

## Water Quality Model

EPANET water quality solver is based on the Lagrangian method, which is the most efficient time-driven method that tracks the fate of individual water segments moving within the pipe and mixing at nodes/junctions (Rossman et al., 2020). The governing formulae for the water quality solver are based on mass conservation principles and reaction kinetics (Hatam et al., 2018). The equations include advective flow in pipes, mixing at junctions, and reaction kinetics as discussed in this section.

### *Advective flow in pipes*

In advective transport, it is assumed that the substance dissolved in fluid travels at a similar mean velocity as that of the respective fluid along the length of the pipe while reacting (growth or decay at a particular rate) at the same time. Longitudinal dispersion is ignored which means no mixing of mass occurs among adjacent water parcels flowing downstream.

$$\frac{\partial C_i}{\partial t} = -u_i \frac{\partial C_i}{\partial x} + r(C_i) \quad (18)$$

where:

$C_i$

= concentration (mass/volume) in pipe  $i$  as function of distance  $x$  and time  $t$

$u_i$  = flow velocity (length/time) in pipe  $i$

$r$  = rate of reaction (mass/volume/time) as a function of concentration

### *Mixing at nodes (pipe junctions & Tanks)*

Fluid mixing at junctions from different pipes is assumed to be complete and instantaneous. As a result, the water outflow concentration is the sum of all inflow concentrations from different pipes. The expression can be written as for a particular node  $k$ : (Rossman et al., 2020).

$$C_{i|x=0} = \frac{\sum_{j \in I_k} Q_j C_{j|x=L_j} + Q_{k,ext} C_{k,ext}}{\sum_{j \in I_k} Q_j + Q_{k,ext}} \quad (19)$$

where:

$i$  = link with flow leaving node  $k$

$I_k$  = set of links with flow node  $k$

$L_j$  = length of link  $j$

$Q_j$  = flow in link  $j$

$Q_{k,ext}$  = external source flow enetering the network at node  $k$

$C_{k, ext}$  = concentration of external flow enetering at node  $k$

$C_{i|x=0}$  = concentration at start of link  $i$

$C_{i|x=L}$  = concentration at end oflink  $i$

Mixing at the tanks follows mass balance equations depending on the type of mixing adopted. Common mixing methods include; complete and two-compartment mixing, and plug flow types first in first out (FIFO), and last in first out (LIFO) (Rossman et al., 2020).

### ***Bulk flow reactions***

The rate of reactions between a substance in the fluid as they move along the pipe or reside in storage facilities can be described as power functions of respective concentrations (Rossman et al., 2020).

$$r = K_b C^n \quad (20)$$

where  $K_b$  = bulk reaction constant,  $n$  = reaction order

In the presence of limiting concentration on substances decay or growth, the expression for the rate can be described as

$$R = K_b (C_L - C) C^{n-1} \quad \text{for } n > 0, K_b < 0 \quad (21)$$

$$R = K_b (C - C_L) C^{n-1} \quad \text{for } n > 0, K_b < 0$$

where  $C_L$  = limiting concentration

Different reaction rate equations can be applied, and these include “*first-order decay*” mostly used to model substances such as chlorine. By-products of water disinfection such as trihalomethanes can be modeled by first-order saturation growth decay rates. Second-order decay, two components, is used for modeling two substance that reacts forming a product. It is assumed that the depletion rate of one reactant is proportionate to the two remaining substances' product. Others include Michaelis-Menton decay kinetics and zero-order growth kinetics. The latter is used for modeling water age (Rossman et al., 2020).

### ***Pipe Wall reactions***

Pipe wall reactions represent reactions between fluid substances and substances on pipe walls such as rust or biofilm formed on the pipe walls. The surface area of the wall and the rate at which mass is transferred from the bulk fluid to the pipe wall and vice versa affect the overall reaction rates. The coefficient of mass transfer can be used to represent the rate and is dependent on molecular diffusivity or reactants and the flow's Reynold number

(Rossman et al., 2020). An example of a first-order kinetic rate of reaction is represented as

$$r = \frac{2k_w k_f C}{R(k_w + k_f)} \quad (22)$$

where:

$k_w$  = wall reaction rate constant (length / time)

$k_f$  = mass transfer coefficient (length/time)

$R$  = pipe radius

For zero-order kinetic, the reaction rate is less than the mass transfer hence

$$r = (K_w, k_f C)(2/R) \quad (23)$$

where  $K_w$  = now has units of mass / area / time

Equations 1, 2, and various equations for mixing in tanks, when applied to a full network, forms a set of DAEs with time-dependent coefficients which are solved for initial concentration at pipe (including junction concentration where the pipe is attached) and concentration in every storage reservoir.

### 2.2.3. EPANET MSX

EPANET MSX is an extension of the EPANET 2 water quality solver and has the additional capability to model multiple species unlike in other EPANET versions (Seyoum & Tanyimboh, 2017). It can model the interactions between different species in the bulk flow as well as in the pipe walls by providing solutions to a set of DAEs provided by the user (Hatam et al., 2018).

### 2.2.4. Water network management (Aquis).

The hydraulic modeling tool is capable of simulating water flow and pressure in the WDN. Aquis, unlike other models, can analyze and track current conditions in real-time, allowing operators to make better and more informed decisions to optimize production and improve economic prospects (CTI resources, 2021). A stable and fast numerical engine is utilized for simulations in the model hence complex and large networks can be analyzed quickly and accurately. The dialog boxes and graphical tools can be used to enter setup data, and the results of the simulation can be shown in reports, tables, and charts, (Schneider Electric, 2021). The tool can allow for integration with real-time monitoring data from “Supervisory control and data acquisition (SCADA)” systems as well weather data to predict the current and future WDN’s performance and patterns of consumption. Similarly, the ability to incorporate Geographical Information Systems (GIS) provides the ability to view different areas and zones, and sections of WDN (CTI resources, 2021). The model can track water quality parameters in real-time such as chemical residuals, taste & odor, and water age (CTI resources, 2021; Schneider Electric, 2021).

### 2.2.5. Quantitative Microbial Risk Assessment (QMRA)

One purpose of “Quantitative Microbial Risk Assessment (QMRA)” is to characterize the health risk related to microbial drinking water contamination considering raw water

quality, water treatment strategies, exposure (who consumes the water and how), and consumers' susceptibility to illness (WHO, 2016). A huge benefit of QMRA is that it enables the user to simulate different scenarios with for example high pathogen load or scenarios with sub-optimal functioning. This makes it possible to analyze how these changes in the system affect the outcome. It makes it also possible to find the optimal solution for a treatment plant, to design or maintain it as stable as possible against changes and unexpected events (Pettersson et al., 2017).

The workflow for QMRA is described in Figure 2.1 below. It is derived from the flowchart WHO, (2016) with additional adjustments for it to include also the decision process. A modified workflow is believed to better reflect how the components are related, and exclusion of “secondary transmission and immunity” that is not a part of drinking water assessment in WHO Guidelines. The components of the flowchart are described in more detail in the paragraphs below.

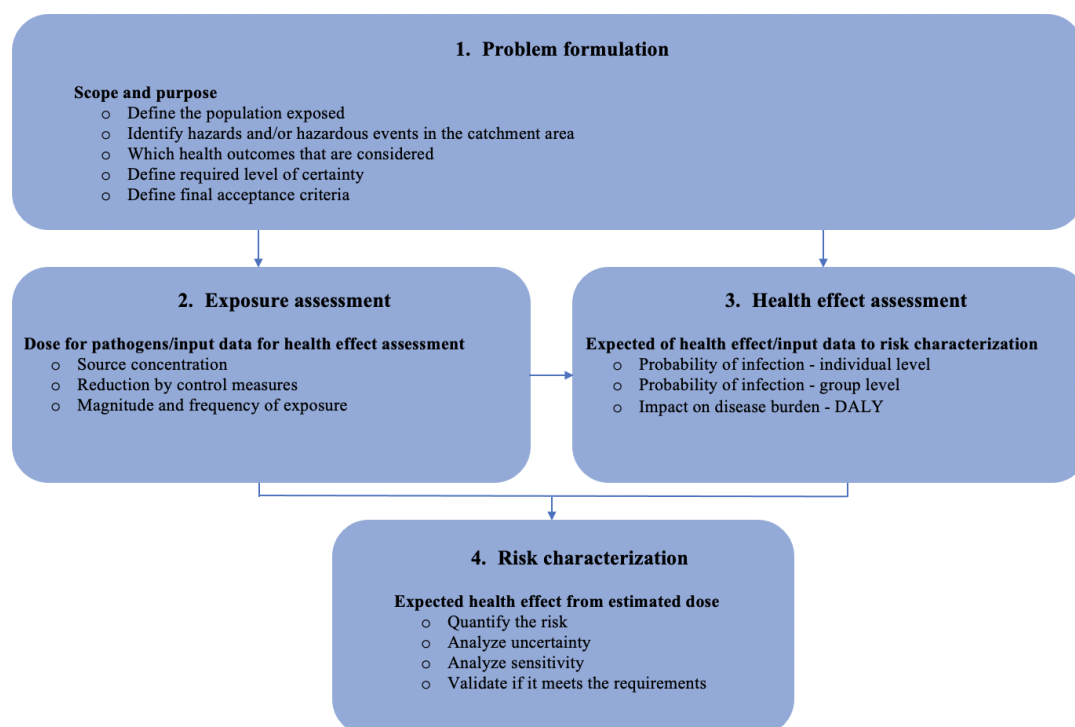


Figure 2.1: Flowchart QMRA derived from WHO Guidelines (WHO, 2016).

## Step 1 – Problem formulation

To start with, it is necessary to develop a plan for the analysis, including its scope and purpose, to ensure that the QMRA accomplishes the analysis's objective. To generate a useful analysis, it is of importance to determine the population that is exposed. It is also important to identify hazards/hazardous events in the catchment area as well as what health outcomes should be considered in the analysis (WHO, 2016).

The hazard identification includes determining what pathogen group(s) are of interest for the analysis, so-called reference pathogens. Aspects to take into account when deciding this can be what pathogen and/or pathogen group that is most relevant for the users, which pathogen are most likely to occur and cause disease, and how persistent the pathogen is. Another important factor to take into account is what data is available in terms of measured data, available scientific literature e.g., dose-response models. When there is no dose-

response relationship defined for the specific pathogen, another model in the same pathogen group is used, often the worst case (WHO, 2016). The relevant pathogen group and related dose-response models are defined as part of the problem formulation as preparation for and to secure consistency in the following steps “Exposure assessment” and “Health effect assessment” (WHO, 2016).

WHO (2016) recommends that for drinking water that can lead to human intestinal illness there should be one pathogen for each group that represents the others, meaning that if every pathogen in each group is fine, all other pathogen is also below the accepted risk level. Both WHO Guidelines for drinking water quality (GDWQ) (WHO, 2017) and WHO Guidelines for the safe use of wastewater, excreta, and greywater (GWEG) (WHO, 2014) recommend including *Rotavirus* from the pathogen group viruses, *Campylobacter* from the group bacteria's, and *Cryptosporidium* from the group protozoa's.

The identification of hazardous events includes determining what events should be included in the analysis. This is based on what pathogens are determined to be included based on the specified aspects in the hazard identification (WHO, 2016).

The health outcomes should be specified in relation to the risk assessment's purpose. Examples of parameters to consider can be the probability of infection, both on individual and group level, as well as Disability Adjusted Life Years (DALY's) which is a measure that includes all aspects of illness and infection of the health outcome (WHO, 2016).

It is argued that it is also necessary to set the requirements for the risk characterization already as part of the initial planning. Therefore, two aspects have been added to the problem formulation, “Define the required level of certainty” and “Define final acceptance criteria”.

It is relevant to clarify the level of uncertainty that the decision-makers require because this will impact and steer the quality of input data that will be needed and thus, facilitate planning and execution of the risk assessment. It is also valid to define the acceptance criteria already in the problem formulation for a similar reason that it helps direct and define the working process in the risk assessment.

The initial requirements for certainty and acceptance criteria will most certainly need to be reviewed and sharpened as more learnings are made through the cause of the process.

## **Step 2 - Exposure assessment**

WHO (2016) defines the exposure assessment as an estimation of the extent and frequency of the identified reference pathogen in each contamination event. This aims to incorporate both the exposure dose and the dose-response relationship. It can be divided into three steps: define exposure pathway, quantify each component of exposure pathway and characterize the exposure, see Figure 2.2 for how they interact.

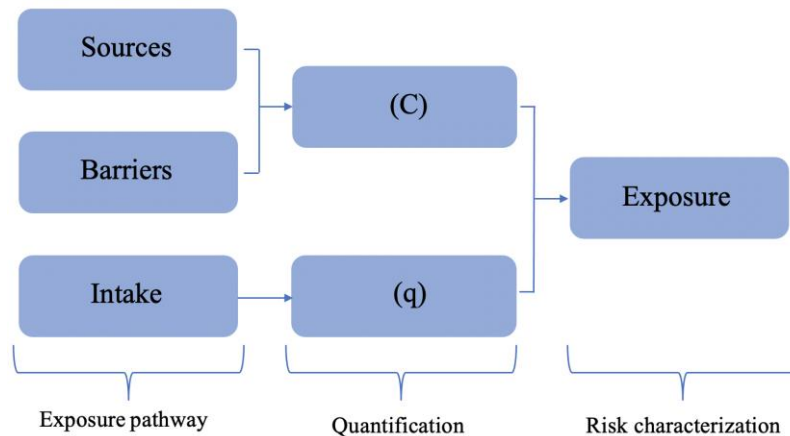


Figure 2.2: Flowchart describing how pathway links to exposure dose derived from WHO Guidelines (WHO, 2016).

The exposure pathway includes qualitative and quantitative characterization for how pathogens reach the end consumer. It contains three components: sources, barriers, and intake, where sources and barriers together will determine the concentration (C) of pathogens the end consumer is exposed to and intake describes the quantity consumed (q) (WHO, 2016).

Sources refer to the raw water sources that may be contaminated with pathogens and require treatment (barriers). Sources include surface water (rivers and lakes) and groundwater. The pathway describes how the source could become contaminated under various conditions and by pathogens. Surface water usually requires more treatment than groundwater (WHO, 2016).

Barriers describe the different means applied to reduce pathogen content in the water to reach the consumer, e.g., water treatment plants or actions in the catchment area (WHO, 2016).

Intake describes where and how, how much and how often the end consumer consumes the water. Where and how defines if it is tap water or well water for drinking or food preparation, i.e., intentional consumption or from swimming i.e., unintentional consumption. How much and how often will define the q parameter for the eventual risk characterization (WHO, 2016).

When the pathways are defined it is time to quantify the pathogens in the source. When determining the concentrations of the pathogens it is necessary to be aware of how the concentrations are determined, how the models used works, and what simplifications and limitations it has. The available data is often insufficient, that is why it is important to include and combine site-specific and literature data. Examples of how to handle these situations when enumeration data is not available, data from indicator organisms are used instead (WHO, 2016).

It is often preferred and recommended to address the impact of the barriers on the pathogen level (C) rather than attempting to directly measure it. There are two reasons for this: firstly, there is often an inherent difficulty to obtain accurate and reliable data of pathogen concentration that will cover relevant variations, Secondly, risk assessment is frequently

used to determine the efficacy of existing barriers or to design adequate barriers (WHO, 2016).

The water source is what determines what control measures are required. As an example, 50% of the water source for drinking water in Sweden originates from surface water (Swedish Civil Contingencies Agency, 2021) which requires control measures in form of conventional treatment (coagulation, flocculation, filtration), disinfection, and the distribution network for control measures. The concentration of pathogens (C) can enter in all these control measures as well as in the raw water source (WHO, 2016).

The characterization of the exposure is then defined in terms of the product of pathogen concentration at which the end consumer is exposed to, and the quantity consumed, as described in equation 24 (WHO, 2016).

$$D = C \cdot q \quad (24)$$

*where*

*D = Exposure dose*

*C = Concentration of pathogen that the end consumer is exposed to*

*q = quantity consumed by end consumer*

### **Step 3 - Health effect assessment**

Four parameters are used to describe the effect on health which are later used in the risk assessment/compared to the defined risk levels (WHO, 2016):

- Dose-response
- Probability of illness and sequelae
- Disease burden (DALY)
- Secondary transmission and immunity

The last one, “secondary transmission and immunity”, is for drinking water assessment not included in the WHO guidelines and will therefore not be considered further in this paper (WHO, 2016).

#### ***Dose-response***

Dose-response is the relation between the pathogen levels and the probability of it causing illness. Dose-response assessments make use of published data in the literature on specific species and their impact on human health. It is therefore always a level of uncertainty when these data are applied to another strain of microbes that may have a different virulence and another population group with different resistance to infection (WHO, 2016).

The dose-response relation is most often assumed to follow an Exponential-Poisson distribution. With  $r$  = the probability for an infection by a single hit,  $c$  = concentration of pathogens and  $V$  = volume consumed, the probability for infection by a single hit can be written as equation 25 below (WHO, 2016). This is further used in equation 28 to get an annual infection rate.

$$P_{inf}(c \cdot V) = 1 - e^{-r \cdot c \cdot V} \quad (25)$$

There are several modifications and improvements of this relation taken into consideration the variability of infection probability for the pathogen as well as different health status and immunity of the population. One commonly used probability function assumes that  $r$  follows the beta-distribution with parameters  $\alpha$  and  $\beta$  ( $r \sim B(\min, \max, \alpha, \beta)$ ). The commonly used probability function to describe a variable  $r$  is as equation 26 below (WHO, 2016).

$$P_{inf}(c \cdot V; \alpha, \beta) = 1 - {}_1F_1(\alpha, \alpha + \beta; -c \cdot V) \quad (26)$$

${}_1F_1$  is a hypergeometric distribution which is a discrete probability distribution. The notation index 1 of each side denotes the probability for one successful hit (i.e., the dose causes illness of the host) in one attempt (i.e., the host has once ingested the dose  $c \cdot V$  (Taghia, 2014). Whereas  $r$  has the variability according to a beta distribution. In data published literature, it can often be found that  $r$  is a constant or if variable the parameters  $\alpha$  and  $\beta$ . According to the beta-distribution, the expected value for  $r$  is defined as  $r = \frac{\alpha}{\alpha + \beta}$  (WHO, 2016).

If  $\alpha \ll \beta$  and  $\beta \gg 25$  equation 26 can be approximated by equation 27 below:

$$P_{inf}(c \cdot V; \alpha, \beta) = 1 - \left(1 + \frac{c \cdot V}{\beta}\right)^{-\alpha} \quad (27)$$

Which is a linear relation between  $P_{inf}$  and  $c \cdot V$ .

If the constraints on  $\alpha$  and  $\beta$  are not met equation 26 can be approximated by a linear dependence using  $r = \frac{\alpha}{\alpha + \beta}$  with  $r$  as a coefficient. This relation is valid for an average dose level of microorganisms  $< 0.3$  (WHO, 2016).

### ***Probability of illness and sequelae***

The definition of illness is when an infection develops into a disease, while sequelae are secondary conditions of disease following a period of illness or infection (WHO, 2016).

The probability for infection over a time period takes into account all exposures in that period. The time chosen is often one year. The annual probability of infection is calculated by equation 28 below (WHO, 2016):

$$P_{Annual\ infection} = 1 - \prod_{i=1}^m (1 - P_{inf_i})^{N_i} \quad (28)$$

Where  $m$  represents the number of type of events, e.g., bad raw water due to contamination of pathogens or suboptimal functioning in the WTP including events with non-contaminated water (normal operation).  $N_i$  is the number of days per type of event and  $P_{inf_i}$  is the probability for single-dose infection causing illness per type of event (WHO, 2016).

The reference value for annual probability is  $10^{-4}$  persons infected per year while for the daily infection it is  $10^{-6}$  persons infected per day (WHO, 2017).

### ***Disease burden (DALY)***

The burden of disease is a way to quantify the impact of illness. One way to do this is using Disability-Adjusted Life Years (DALYs). The acceptable risk for DALY is according to WHO defined as  $10^{-6}$  (WHO, 2017). DALY is used in international statistics to describe and quantify a wide range of situations and conditions that may cause illness. It makes it possible to quantify and compare the effect of quite different health-impacting situations like diseases, interventions, preventive measures, environmental and social situations on human health (Havelaar et al., 2000; WHO, 2003).

DALY is defined as the “*sum of years of life lost (YLL)*” and “*years living with a disability*” (YLD). YLD is weighted by a factor ranging from 0 to 1 to reflect how severe the disability is. (Havelaar et al., 2000; WHO, n.d.). “Both YLL and YDL are calculated by an accumulation over all relevant diseases (*i*)”, where:

YLL is calculated by equation 29:

$$\sum_i d_i \cdot e_i^* \quad (29)$$

where:

$d_i$  = Number of deaths due to a particular disease

$e_i^*$   
= The standard life expectancy at the age of death due to that disease

The life expectancy is consideration taken to age, gender, region, and year of death using the UN life expectancy data.

YLD is defined by equation 30:

$$\sum_i N_i \cdot L_i \cdot W_i \quad (30)$$

where:

$N_i$  = Number of persons affected by a non  
– lethal disease or disability

$L_i$  = Duration of this disease

$W_i$  = A measure for its severity

### **Step 4 - Risk characterization**

The risk characterization process combines the data from steps 2 and 3 to produce an estimate of total risk. The result can be presented as deterministic (a single value) or probabilistic (by a distribution) depending on what input data is used and how the results should be presented. The presentation of the data and which parameters are included are all determined in accordance with the risk assessment's purpose and the way it was defined in the problem formulation (WHO, 2016).

Common parameters used to present the risk assessment can be DALY, probability of illness, or probability of infection which then can be compared to the criteria value determined in the problem formulation. The parameters chosen can be presented in a multitude of ways, e.g., the annual mean value or daily time series. Sensitivity analysis can

be applied to explore the impact of variations for the assumptions and also to account for the uncertainty in input data (WHO, 2016).

### 2.3. Pathogens

This section includes short descriptions of the characteristics of the pathogens that were adopted for this study.

#### 2.3.1. Indicator organisms

An indicator organism is used to indicate if there is fecal contamination in the water, which may include pathogens (Swedish Institute for Infectious Disease Control, 2011). The indicator organism in itself may not be a pathogen but should occur simultaneously with pathogens. Other wanted properties for an indicator organism are that it does not propagate or is pathogenic and that it mimics the survival mode of the pathogen, and that this behavior is the same for all types of water. Another very important factor is that it should be easy to detect, even at low concentrations, as well as that it should be cheap, quick, and reliable. In reality, however, it has been proven that these requirements are often met only to a limited extent (Arvidsson, 2019).

WHO Guidelines (WHO, 2017) recommend using *E. coli* as an indicator organism. While *E. coli* in itself normally is not a pathogen but occurs in the intestinal tract it is frequently used as an indicator organism for other pathogens water (CDC, 2014; Victor et al., 2021). *E. coli* is a bacterium that is mainly of fecal origin from animals and humans, where it is found in high concentrations. They have survival in water ranging between a week and a couple of months and respond to disinfection, temperature variations, and other environmental conditions. These properties all together make them very suited as an indicator organism for fresh contamination by pathogens of the same origin (Arvidsson, 2019).

#### 2.3.2. Cryptosporidium

*Cryptosporidium* is a protozoon that can survive for long times in water and may cause intestinal illness with diarrhea and sometimes even vomiting (Arvidsson, 2019). It is highly contagious since it can cause illness at doses as low as 10 oocysts (WHO, 2017). It belongs to the group of protozoans that are most resistant to chemical disinfectants such as chlorination. However, since they are quite large ( $> 2\mu\text{m}$ ) they can be removed with physical processes, such as filtration (WHO, 2017).

WHO Guidelines (WHO, 2017) recommend both *Giardia* and *Cryptosporidium* be used as reference pathogens since there are dose-response models for both of them. *Giardia* which is another pathogen in the group protozoa more often infects people. But, since *Cryptosporidium* is smaller than *Giardia* WHO (2017) and therefore harder to remove combined with that it is more persistent in waters and also more resistant to chemical disinfectants, it is chosen as a reference pathogen for this analysis.

It is important to observe that absence of an indicator organism (*E. coli*) does not secure that the water is free from *Cryptosporidium*. This is because *Cryptosporidium* is more persistent than *E. coli* and exhibits a longer survival in water (Swedish Food Agency et al., 2017; WHO, 2017), especially at low temperatures (Swedish Institute for Infectious Disease Control, 2011).

### 2.3.3. Norovirus

*Norovirus* is the pathogen that is the most common cause for GII (Swedish Public Health Agency, 2018) with genotype G2 being most harmful (Aspevall et al., 2014). *Norovirus* is highly contagious with an infectious dose as low as 1-100 microorganisms (Swedish Public Health Agency, 2018). According to Hassan & Baldrige, (2019), less than 20 microorganisms of *Norovirus* can cause infection. *Norovirus* is also easily transmitted and causes, like *Cryptosporidium*, vomiting, and diarrhea (Hassan & Baldrige, 2019).

Chemical disinfectants, like chlorine, as well as boiling, are effective controls to remove viruses from water, while filtration is not (CDC, 2009). *Norovirus* can survive in water for more than a month and it is also concluded in a study on viruses in water by the Swedish Public Health Agency (2018) that since *E. coli* and *Norovirus* survival in water differs, an estimate of *Norovirus* prevalence based on *E. coli* levels may be misleading.

The Swedish Public Health Agency (2018) claims that due to climate change there will be an increasing number of waterborne outbreaks where *Norovirus* is the one most concerning. This is concluded that the relationship between the occurrence of *Norovirus* and extreme rain events has been demonstrated.

WHO (2017) identifies *Norovirus* as one potential reference pathogen for the group of viruses and has dose-response models available. It was thus adopted for this study based on the WHO conclusion and the concern about its growing importance.

### 2.3.4. Campylobacter

*Campylobacter* is a bacterium that causes diarrhea worldwide with a low infectious dose (<1000 organisms) compared to other bacteria, where *Campylobacter jejuni* is the species of the group making most people ill (WHO, 2017). *Campylobacter* occurs in many different areas in the environment where one of them is water. It has been proven that the amount of water strongly correlates with rainfall, water temperature, and waterfowl (WHO, 2016).

Its resistance against disinfection is low (Ct99 of <1 min mg/L), has dose-response models that fit both clinical and outbreak data. Like *Cryptosporidium* its survival in water, especially cold, is long (WHO, 2016).

Consumption of food is the most common reason for illness caused by *Campylobacter*, but drinking water also has a high significance where the cases increase. Since *Campylobacter* originates from fecal and that the resistance against disinfection is low, *E. coli* is a good indicator organism to determine the presence or absence of *Campylobacter* (WHO, 2016).

This together makes *Campylobacter* a good option to be used as a reference pathogen for the group bacteria.

### 2.3.5. The ratio between *E. coli* and pathogens

Several studies reported the difficulty to define a typical ratio between *E. coli* and pathogens, like *Cryptosporidium* and *Norovirus* (Lalancette et al., 2014). Lalancette et al, (2014) tested raw wastewater, water from agriculture runoff, and secondary treated wastewater to evaluate the ratio between *E. coli* and *Cryptosporidium* (Ec/Cr). Lalancette et al, (2014) also reported a range for agriculture run-off water and treated wastewater

between  $4.9 \cdot 10^5$  –  $8.2 \cdot 10^6$  for the ratio. For raw wastewater, there was no correlation, but the Ec/Cr ratio was always safely higher than  $8.2 \cdot 10^6$  which suggests that using the range above will not lead to a risk of underestimating *Cryptosporidium* levels.

It is frequently reported that the quantitative relation between *E. coli* and *Norovirus* cannot be established with reasonable accuracy (Sharp et al., 2021; Tian et al., 2017; Victor et al., 2021). In the lack of this, reported literature data on typical values for *E.coli*, *Norovirus*, and *Cryptosporidium* in wastewater was used.

#### **2.4. Summary of Hydraulic modeling and QMRA**

Contamination of water in the WDN has been associated with various disease outbreaks and the resultant GII. Studies in various parts of the world, as demonstrated by the literature, have indicated an increase in the proportion of GII cases in recent times. To be able to provide effective remediation measures it is necessary to understand and quantify the risks posed by intrusions (pathogens and other substances) into the WDNs. Due to the location of WDNs in the water supply chain, at the discharge end, it is impossible to detect contamination in time for remediation using conventional measurement techniques at the demand nodes (draw-off points) prompting the adoption of different solutions.

Hydraulic modeling coupled with water quality modeling is one such solution that has been adopted, which can facilitate tracking the distribution of contaminants from the entry to the usage points. Various interactions that reduce (decay) or increase (growth) of contaminants can be modeled as well giving the possible concentration in a specific time and at a specific area of the WDN. Only distributions of contaminants in the WDN are possible with hydraulic and water quality modeling. To be able to determine impacts or risks associated with pathogen intrusion, a quantitative microbial risk assessment program is necessary. Combining QMRA, hydraulic, and water quality modeling makes it possible to quantify risks associated with loss of integrity in WDN and quantify annual infection risk and estimate the disease cost burden.

The most contributing factor for the intrusion to occur is the loss of hydraulic integrity, especially poor hydraulic gradient, in the presence of compromised physical integrity such as pipe breaks, cracks, and holes. In this study, a hydraulic model developed for WDN south of Sweden was used with some of the tools described in Section 2.2 to simulate low pressure conditions and quantify the potential health impacts of pathogen intrusion. Vulnerable areas in the network were analyzed and mitigation measures proposed such as real-time monitoring using sensors.

Illness caused by drinking water contaminated by pathogens is a globally occurring problem approached both with methods to avoid contamination and purify the water as well as studies to understand survival conditions and contagiousness of the pathogens. Pathogens are a very broad group of microorganisms and to manage that, numerous studies have identified suitable microorganisms that are considered reasonably representative and are possible to monitor. These reference organisms are frequently used to characterize the pathogen load in drinking water.

### 3. Method

The section describes the project infrastructures, materials, and modeling procedures adopted for this study.

#### 3.1. Study area description

This project considered a section of WDN in the south of Sweden and due to security reasons, the exact location was not specified further. All data in this project was given from the utility for this specific network, including EPANET data files for estimating hydraulic characteristics (flow, pressure, and nodal demands), shapefiles with geodata, and PENZD-files (Point, Easting, Nothing, Elevation, Description) for locating fire hydrants and nodes on a map with Civil 3D tool.

The WDN has comprised a total of 1,167 nodes (junctions). The network was supplied from a reservoir and was comprised of 1,185 links (pipes) totaling 45.7 km of piping of varying materials. The pipe network included 250 mm diameter main pipelines to 25 mm diameter distribution pipelines. The WDN could serve approximately 4,800 people equivalents with a total demand of 769 m<sup>3</sup> per day (8.9l/s). Prevalent demand patterns of this project area were apartment housing, detached housing, and industrial usage.

This WDN just like other distribution networks in developed countries faces the challenge of aging and compares well to the national statistics associated with this problem. Aging is the cause of leakages and to some extent pipe breaks. According to the Swedish water works association, breaks and leaks are estimated to occur 5000 times in any given year (Swedish Water, 2015). Leakage alone accounts for 10-15% of the drinking water production losses.

For this project, according to the distribution data from the project area, leakage accounted for 16% of the production losses in 2020. The value was observed to closely relate to the national statistics. The leakage has been used to prioritize the renewal areas, with the most prevalent leak area given priority. However, due to increasing renewal needs, repair needs have consequently suffered. In the presence of pressure drops in the WDN, withholding repair needs leads to increased risks of pathogen intrusion (Swedish Water, 2015). Changing climate conditions are expected to contribute to extreme weather conditions such as torrential rains and flooding, which can lead to submerging of pipes thus increasing pathogen intrusion rates in event of lower pressure situations. The WDN network is assumed to have most of its pipes approximately 0.15 m below the groundwater level hence faces increased risks of intrusion. With most of the pipes within the project area being within the same trench as the sewer pipelines, a higher groundwater level can increase the risk of pathogen intrusion from the sewer pipelines to the drinking water pipelines. Studies indicate 83% of Sweden's drinking water and sewer pipes are within the same trenches of which 20% are below the groundwater level (Rikard Dryselius, 2013).

The most likely low-pressure events, necessary for intrusion, in the project area, were anticipated to be pumping station failures and high demand due to emergency fires. For intrusions leading to the onset of GI, disease-causing pathogens must be present within the surrounding of the WDN (Rikard Dryselius, 2013). In Sweden, 83% of drinking water pipes are located within the same trench as the sewer pipelines hence this act as a potential source of pathogens. Pathogens *Campylobacter*, pathogenic *E. Coli*, *Salmonella*, *Shigella*,

*Norovirus*, *Cryptosporidium*, *Entamoeba histolytica*, and *Giardia* have been associated with drinking water outbreaks since 1980 (Rikard Dryselius, 2013). Reference pathogens were used in this study and are described in Section 2.3.

### 3.2. Modeling process

To accomplish the study's objective, the project was implemented in four phases, as illustrated in Figure 3.1. The first phase involved hydraulic simulation of WDN in three different scenarios (more details in section 3.4):

1. Normal operating conditions (scenario 1)
2. Suboptimal operation due to a pump failure in the system (scenario 2)
3. Extreme water consumption due to a fire emergency (scenario 3)

The second phase involved the determination of pathogen intrusion during low pressure conditions for Scenarios 2 and 3. In the third phase, water quality simulation was performed for scenarios 2 and 3, and pathogen distribution in the WDN network was determined. In the fourth phase, a QMRA was used for determining the risk posed to human health by pathogen intrusion in the WDN.

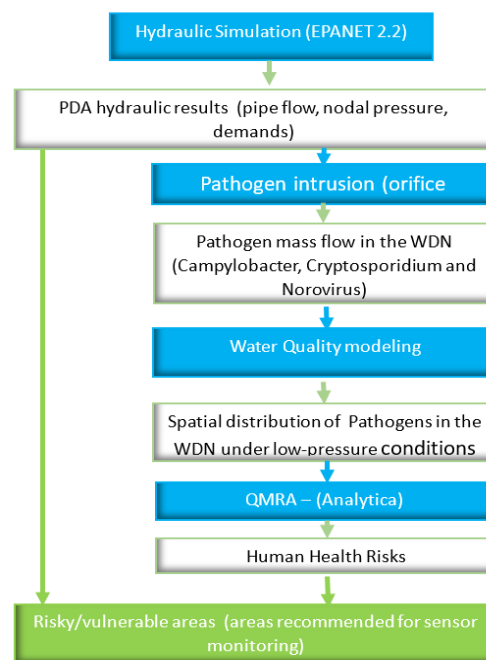


Figure 3.1: Modeling process.

### 3.3. Hydraulic simulation

For this study, an already built model was used representing a section of an existing WDN south of Sweden. An EPANET input data file was provided for the simulations. EPANET 2.2, described in Section 2.2.2, was used throughout the simulations. This version of EPANET was considered due to its capability for performing both “Demand-Driven Analysis (DDA) and Pressure-Driven Analysis (PDA)” (Rossman et al., 2020). In EPANET, the critical setting is the headloss model adopted. The three commonly used models for calculating headloss in EPANET include “Hazen-Williams (H-W), Chezy-Manning (C-M), and Darcy-Weisbach (D-W)” as described in Table 2.2 (Sami, 2018).

They all follow Equation 1 which when minor losses are ignored it is simplified as illustrated in Equation 31.

$$h_L = Aq^B \quad (31)$$

where  $h_L$  = friction headloss in pipes

$A$  = resistance coefficient

$q$  = flowrate (volume/time)

$B$  = flow exponent

D-W headloss model was adopted in EPANET for these simulations and other hydraulic parameters were set as shown in Figure 3.2 (a). The setting for the PDA demand model can be observed from Figure 3.2 (b) while for DDA in Figure 3.2 (c). With the PDA model, pressures were set for 0 and 20 m for minimum and required pressure respectively while for the demand model, they do not have any effect on demand output, however, 0.1 is set for desired pressure in DDA to avoid numerical calculation error.

Hydraulics Options	
Property	Value
Flow Units	LPS
Headloss Formula	D-W
Specific Gravity	1.000000
Relative Viscosity	1.000000
Maximum Trials	40
Accuracy	0.001000
If Unbalanced	STOP
Default Pattern	1
Demand Multiplier	1.0
Emitter Exponent	0.500000
Status Report	Full
Max. Head Error	0
Max. Flow Change	0

(a)

Hydraulics Options	
Property	Value
Demand Multiplier	1.0
Emitter Exponent	0.500000
Status Report	Full
Max. Head Error	0
Max. Flow Change	0
Demand Model	PDA
Minimum Pressure	0
Required Pressure	20
Pressure Exponent	0.5
CHECKFREQ	2
MAXCHECK	10.000000
DAMPLIMIT	0.000000

(b)

Hydraulics Options	
Property	Value
Demand Multiplier	1.0
Emitter Exponent	0.500000
Status Report	Full
Max. Head Error	0
Max. Flow Change	0
Demand Model	DDA
Minimum Pressure	0
Required Pressure	0.1
Pressure Exponent	0.5
CHECKFREQ	2
MAXCHECK	10.000000
DAMPLIMIT	0.000000

(c)

Figure 3.2: Hydraulic parameters used in EPANET 2.2 (a) general parameters applicable for DDA & PDA (b) PDA model (c) DDA model.

The simulation period adopted was 24 hours, the hydraulic time step was 10 minutes, and the pattern and reporting time steps were set to 1 hour. Report and clock start time was set to 00:00 (midnight).

### 3.4. Scenarios

In this section, low pressure scenarios simulated as well as the normal operation condition are described.

#### 3.4.1. Scenario 1 – Normal operation conditions

Scenario 1 modeled a WDN described in section 3.1. The normal operating conditions included a hypothetical reservoir that reflects the behavior of the pressure in the upstream system, which, in reality, is mainly achieved with a system of pumps. It is set to a head of 78.8 m and varies with a pre-defined pattern (Appendix 1). The normal (base) demand was 8.9 liters governed by several demand patterns. Normal residential water (NRW) pattern 1

(Appendix 2), detached housing and apartment housing pattern 102 (Appendix 3), and industrial use pattern 103 (Appendix 4).

### 3.4.2. Scenario 2 – Low pressure condition (Malfunctioning pump(s))

Sustained low pressure conditions for scenario 2 were achieved by varying the hypothetical reservoir head to simulate the pump operating conditions rather than the use of pump control curves and routines. Ahead of 13 m was used to simulate a pump failure lasting for 5 hours during peak demand. The head was incorporated in the head pattern (hbg\_level) between 11.00 to 16.00 for this scenario as seen in Figure 3.3.

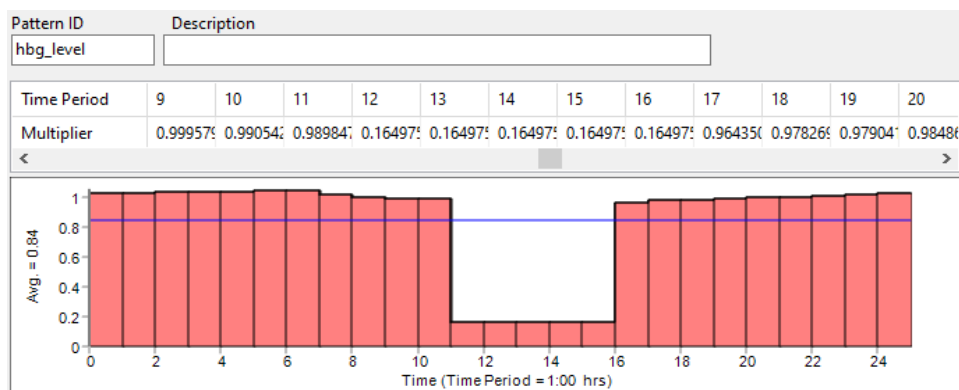


Figure 3.3: Head Pattern for low pressure conditions due to pump failure.

### 3.4.3. Scenario 3 – Fire emergency water supply

The simulation of scenario 3 was done by adding fire-fighting water demand of 20 liters/s to three nodes in the model to represent fire hydrants. The three fire hydrants were used at the same time during three hours between 16:00 to 19:00 (see Appendix 6 for fire hydrant pattern). The fire hydrants were located in the residential area believed to be at the highest risk in the event of a fire emergency. A shapefile with geodata was provided by the water utility and used for locating hydrants in the distribution system. Autodesk Civil 3D was used for accessing the file and the nodes' location data was imported on the file in PENZD (Point, Easting, Nothing, Elevation, Description) format.

## 3.5. Pathogen intrusion

To determine the mass flow of the respective pathogen intrusions in the WDN, intrusion volume was calculated, Section 3.5.1, and used with literature data of pathogens in wastewater coupled with measured representative values of *E. coli* from soil water. The detailed description of the methodology used can be seen in Section 3.5.2.

### 3.5.1. Intrusion volume

The compromised physical integrity in this study was through leakage due to pipe aging. The total leakages acting on the pipe section were assumed to be circular and represent multiple small holes. The total area of the leakage holes was determined using the orifice Equation 32.

$$A_{tot} = Q_{out} \times \frac{1}{C_D \times \sqrt{2 \times g \times \Delta H_{normal}}} \quad (32)$$

where:

$A_{tot}$  = Total area of the hole or breakage with a specific leakage [ $m^2$ ]

$Q_{out}$  = Total leakage volume [ $m^3/s$ ] = 0.0312 l/s \* km

$C_D$  = Constant (Standard value is 0.6 [-]). Depends in the holes "sharpeness"

$\Delta H_{normal}$   
= Difference in pressure inside and outside the hole for normal pressure events

$g$  = 9.81 m/s

The total leakage volume ( $Q_{out}$ ) of 0.0312 l/s\*km represents the total water loss of the produced water, which was 16%. The unit intrusion volume was then calculated as per Equation 33.

$$Q_{int} = C_D \times A_{tot} \times \sqrt{2 \times g \times \Delta H_{pressure\ drop}} \quad (33)$$

where:

$\Delta H_{pressure\ drop}$  = Ground water level in relation to level of water in pipe [m]

$Q_{int}$   
= Intrusion volume of water per time unit due to low or no pressure [ $m^3/s * km$ ]

$\Delta H_{pressure\ drop}$  is the difference in pressure inside and outside of the hole when the pump is shut off. The assumed pressure difference between groundwater level (GW) and center of pipe area ( $\Delta H_{pressure\ drop}$ ) is assumed to be 0.15 m in the affected area during zero pressure events of the pipe. See the definition of pressure due to groundwater in Figure 3.4. Susceptible pipe sections were identified from low pressure zones and the total length in km was multiplied by the unit intrusion rate to determine the intrusion rate per second in liters per second.

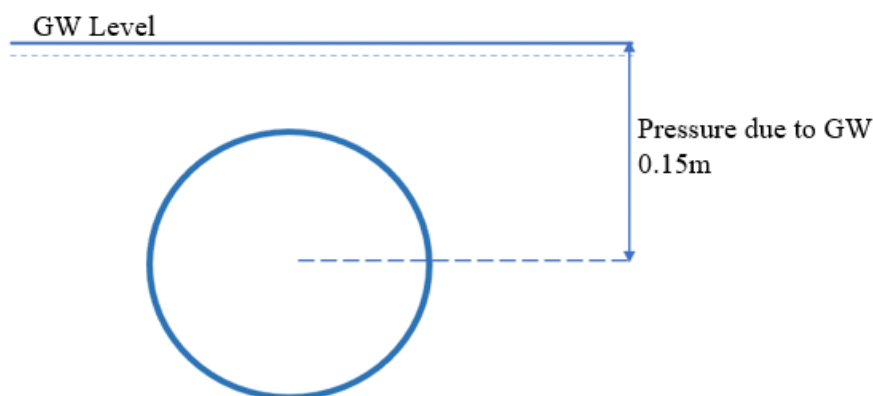


Figure 3.4: Definition of pressure due to groundwater that is included in determining the  $\Delta H_{pressure\ drop}$ .

### 3.5.2. Pathogen concentration

The Swedish Food Agency, Public Health Authority, and Swedish Water reported a normal concentration of *Cryptosporidium* in raw sources as 0.2 oocysts/100 ml. The test period for these results was between 2003-2008 and was conducted from 200 samples. Only 11.5% of them were positive for *Cryptosporidium* (Swedish Food Agency et al., 2017).

In raw wastewater, a range between 2-12 oocysts/100 ml was reported. The wastewater values were a summary of values measured in 5 WWTP located in Sweden. This was substantially lower than reported by other authors (Schönning et al., 2011; Tchobanoglous, 1991). For the analysis in this report a range covering those higher values was selected. Table 3.1 presents summarized mean concentrations of pathogens in wastewater (minimum and maximum), adopted for modeling.

Table 3.1: Summary of concentrations in untreated wastewater for the indicators/pathogens in the analysis used to calculate the ratios *E.coli*/pathogen.

Pathogen	Value [No/100 ml]		Comment
<i>E. coli</i>	10 <sup>7</sup>		Source: (Henze et al., 2002)
<i>Campylobacter</i>	5000		Source: (Henze et al., 2002)
	<u>Min. Value</u> [No/100 ml]	<u>Max. Value</u> [No/100 ml]	
<i>Norovirus G2</i>	307 <sup>1</sup>	7533	Infectious concentration <sup>2</sup> Source:(Dienus et al., 2016)
<i>Cryptosporidium</i>	10	1600	Source: (Schönning et al., 2011; Tchobanoglous, 1991)

<sup>1</sup> To calculate the values for Norovirus data from the WWTP inflow was used for 3 of the total 4 waterworks since there was no detected NoV for one of them.

<sup>2</sup> Assumed that 1 in 1000 NoV is infectious.

The ratio *E.coli*/*Cryptosporidium*, *E.coli*/*Norovirus*, and *E.coli*/*Campylobacter* is calculated from literature data of concentrations in wastewater presented in Table 3.1 above. An assumption is made that the ratio between *E.coli* and the respective pathogen is the same for wastewater as for soil water to be able to estimate the concentrations in soil water. The calculated ratios *Ec*/pathogen for literature data for wastewater are presented in table 3.2 below.

Table 3.2: Calculated ratio between *E. coli* and the pathogen (*Ec*/Pathogen) in wastewater and that is used for estimating concentrations of pathogens in soil water.

Ratio	Value	
	Min	Max
<i>Ec</i> / <i>NoV2</i>	3.26·10 <sup>4</sup>	1328
<i>Ec</i> / <i>Cryptosporidium</i>	1.00·10 <sup>6</sup>	6250
<i>Ec</i> / <i>Campolybacter</i>	2.0·10 <sup>2</sup>	2.0·10 <sup>2</sup>

Rudrappa & Zharkalli (2018) summarized the data of *E. coli* and *total coliforms* in soil water measured at 16 different locations in Gothenburg. The samples were taken during repairs near the drinking water pipe to examine the concentration in soil water around the pipes. They were analyzed both at Chalmers laboratory and Lackarebäck water treatment

plant’s laboratory. The concentration of *E. coli* was extracted from these results. The highest value of *E. coli* in soil water detected was 240 000 CFU/100 ml. This was the reference value used to calculate the concentrations for *Norovirus*, *Cryptosporidium* oocysts, and bacteria *Campylobacter* present within soil water using the ratios in table 3.2 above. The calculated concentration of pathogens in soil water is presented in Table 3.3. These were used for the determination of pathogen intrusion mass flow rates into the WDN under low pressure conditions.

Table 3.3: Calculated pathogen concentration in soil water using ratios between *Ec*/pathogen based on literature data in wastewater.

Pathogen	Concentration [No/L]
<i>Norovirus</i>	1808
<i>Cryptosporidium</i>	348
<i>Campylobacter</i>	1200

### 3.6. Modeling Water quality with EPANET

EPANET 2.2 water quality model described in section 2.2.2 was applied for an “*Extended Period Simulation (EPS)*” for modeling pathogen distribution in the WDN under steady-state conditions for scenarios 2 and 3 (Hatam et al., 2018). The quality parameters in EPANET were set as seen in Figure 3.5.

The hourly pathogen intrusion was injected at the junction (node) as a “Mass booster”. Using Mass Booster means that a fixed mass flow enters the junction momentarily (Rossman et al., 2020). Intrusion patterns (Intrusion 2 and Intrusion 3) were used for Scenario 2 and 3 respectively (see Appendix 7 and 8).

The hour 19:00 was determined to be the most critical time for the water consumption coupled with higher concentrations of pathogens. Therefore, a table was generated for the pathogen variations in all nodes in the system where the concentrations are > 0.01 No/L at this hour. This was assumed to follow a triangular distribution and used in QMRA for risk analysis.

Times Options	
Property	Hrs:Min
Total Duration	24:00
Hydraulic Time Step	0:10
Quality Time Step	0:05
Pattern Time Step	1:00
Pattern Start Time	0:00
Reporting Time Step	1:00
Report Start Time	0:00
Clock Start Time	0:00:00
Statistic	NONE

(a)

Quality Options	
Property	Value
Parameter	E.coli
Mass Units	mg/L
Relative Diffusivity	1.000000
Trace Node	
Quality Tolerance	0.010000

(b)

Reactions Options	
Property	Value
Bulk Reaction Order	0
Wall Reaction Order	Zero
Global Bulk Coeff.	0.000000
Global Wall Coeff.	0.000000
Limiting Concentration	0
Wall Coeff. Correlation	0

(c)

Figure 3.5: Hydraulic water quality modeling parameters used in EPANET 2.2 (a) Time, (b.) Quality, (c) Reactions.

### 3.7. Estimating health risks with QMRA

The method was based on the description of QMRA in section “2.2.5 QMRA” and the assumptions and input for the analysis were summarized below. Figure 3.6 illustrates an overview of the method.

The daily infection probabilities were calculated using a Swedish QMRA tool developed within the Analytica software. In the QMRA tool, the daily consumption volume was set to 1 l/person and the pathogen concentration data used was generated from the EPANET model (Table 4.4 - 4.6). The concentration data refers to a one-hour worst-case scenario and since the QMRA Analytica tool only provides calculations for daily and annual probabilities, a modification was adopted. An assumption was made to calculate the hourly probability of infection ( $P_{inf, hourly}$ ) from the daily probability with the same equation as  $P_{annual}$  (equation 28) with a modification as in equation 33 below.

$$P_{inf, hourly} = 1 - (1 - P_{inf, daily})^{1/24} \quad (34)$$

Still, the guideline value for daily infection,  $10^{-6}$  persons infected, was used as a reference value.

**Purpose:** Evaluate the infection risk for consumers connected to the WDN caused by consuming drinking water contaminated by pathogens due to intrusion caused by low pressure conditions.

**Hazard identification:** The hazard is identified as the risk to get GII sourced by soil water-containing pathogens. The reference pathogens in the soil water were *Norovirus*, *Campylobacter*, and *Cryptosporidium*.

**Exposure pathway:** Intentional ingestion by drinking the water assuming one person drinks 1 l/d.

**Health outcome:** Probability of gastrointestinal illness

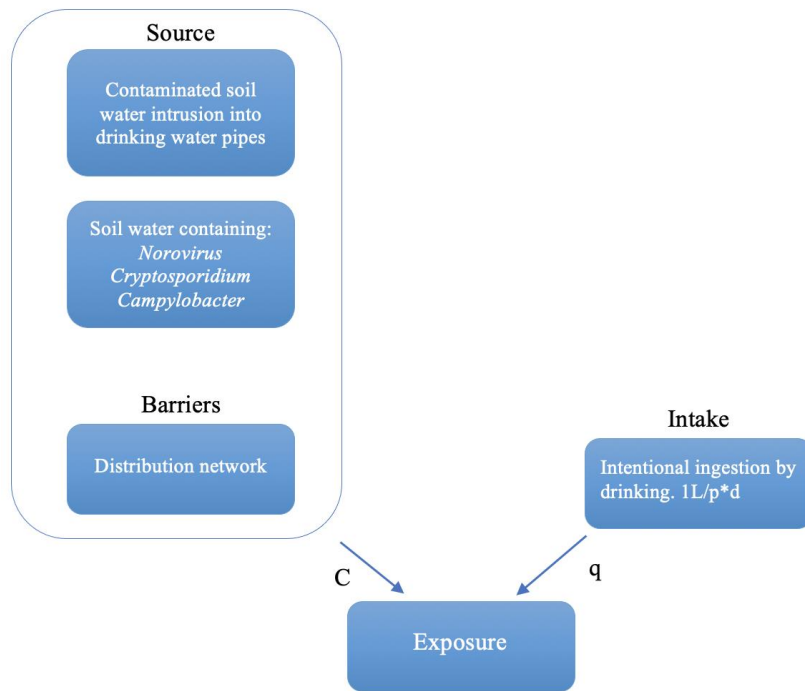


Figure 3.6: Flowchart of the exposure assessment to get the exposure to be able to do the risk characterization. It includes hazard identification, chosen reference pathogens, barriers, and exposure pathways.

## 4. Results

This section describes the outcomes from hydraulic simulations in all three scenarios, pathogen intrusion into the water distribution network in scenarios 2 and 3, water quality simulations for scenarios 2 and 3, and the outputs from QMRA.

### 4.1. Hydraulic characteristic of normal operation conditions

It was observed that when operating under normal conditions the WDN is well designed to meet demands at peak demand times as seen from statistical distribution Figure 4.1 and spatial distribution Figure 4.2 (c-d). Spatial distribution Figure 4.2 (a-b) indicates the systems exceed pressure expectation in some sections during off-peak hours attaining a maximum of 74 m while during peak demand times the pressure requirements (20-70 m) are met as seen in Figure 4.2 (c-d).

To verify the validity of the PDA model used for this study, both the DDA and PDA models were used to run the hydraulic simulation under the same conditions, demand, and pressure. As expected, similar results were obtained as seen in scenario 1. Identical pressure distribution was observed as in Figure 4.2(a) for DDA and Figure 4.2(b) for PDA during off-peak demand while Figures 4.2(c) and (d) show similar demands during peak hours for DDA and PDA models, respectively. Similarly, the demand satisfaction ratios are the same at 100% for both the models as seen in Table 4.1.

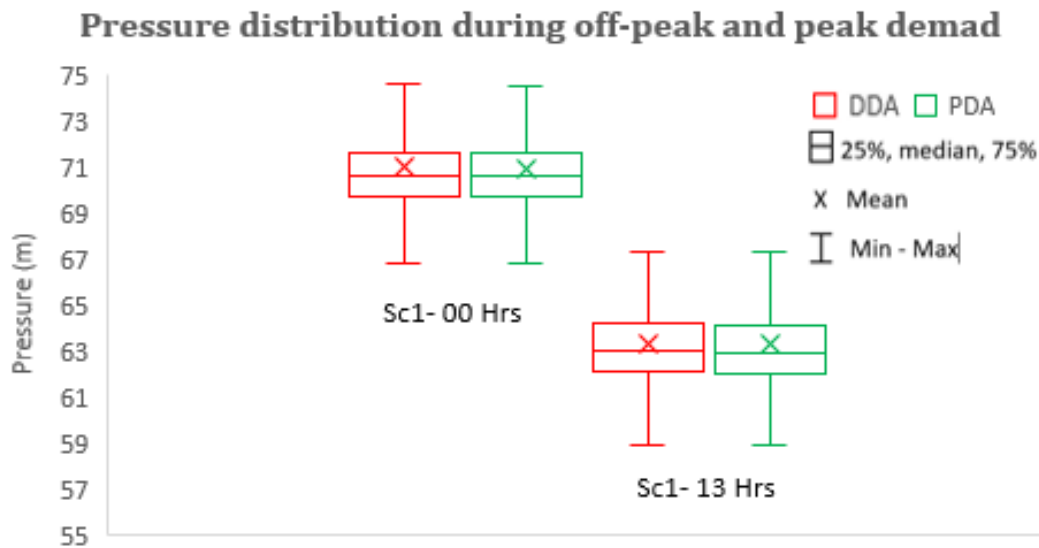


Figure 4.1: Statistical pressure distribution, minimum, median (50<sup>th</sup> percentile), mean, maximum, 25<sup>th</sup> percentile, and 75<sup>th</sup> percentile during off-peak (00:00) and peak hour (13:00) for scenario 1.

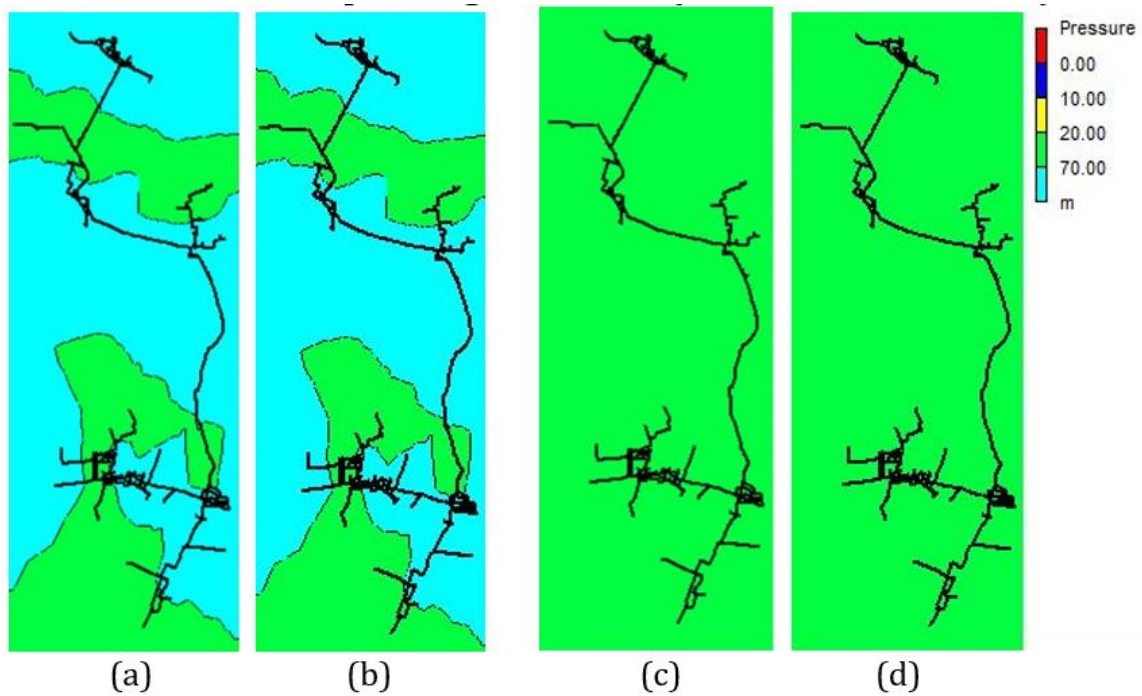


Figure 4.2: Pressure distribution for scenario 1 during off-peak demand for (a) 00:00 DDA and (b) 00:00 PDA and during peak demand (c) 13:00 DDA and (d) 13:00 PDA.

## 4.2. Hydraulic characteristic of low pressure conditions

This section investigates the effects of low pressure on the demand using demand models DDA and PDA.

The demand satisfaction ratio, “The DSR for a node is the ratio of the available demand (under pressure-deficient conditions) to the required demand at that node” (Hatam et al., 2018), was used to observe the behavior of the network when subjected to different pressure scenarios. During normal conditions, the demand satisfaction is met 100 % for scenario 1 while the demand reduces to 32.5 % for scenario 2 and 33.4 % for scenario 3 as shown in Table 4.1. Pressure drop results in reduced Demand Satisfaction Ratio (DSR) indicating the relationship with the hydraulic grade line maintained at the supply point.

Table 4.1: Demand satisfaction ratios for Scenarios 1, 2, and 3.

Description	Sc1	Sc2	Sc3
Total Demand (l/s)	8.910499	8.910499	67.34
Available Demand (l/s)	8.92	8.92	67.34
<b>DSR-DDA</b>	<b>100%</b>	<b>100%</b>	<b>100%</b>
Available Demand (l/s)	8.93	2.9	22.51
<b>DSR-PDA</b>	<b>100%</b>	<b>32.5%</b>	<b>33.4%</b>

As can be observed in Figure 4.3, the same pressure values were identified for scenario 1 using DDA and PDA. As the pressure reduces, exorbitant underestimations are observed in scenarios 2 and 3. For scenario 2, with a DSR of 32.5%, the minimum, median and maximum pressure values were found to be -0.47 m, 3.34 m, and 7.29 m respectively for PDA and -3.79 m, 0.25 m, and 4.57 m for DDA. In Scenario 3, with a demand satisfaction ratio of 33.4 %, the minimum, median and maximum values were -3.13 m, 43.68 m, and 67.26 m for PDA and -770.17 m, -137.99 m, and 65.54 m for DDA. It can be noted that the minimum pressure value from the PDA analysis was -3.13 m for the 2 scenarios as

compared to DDA which had a value as low as -770.17 m highlighting the extent of the pressure underestimation by this model in low pressure conditions.

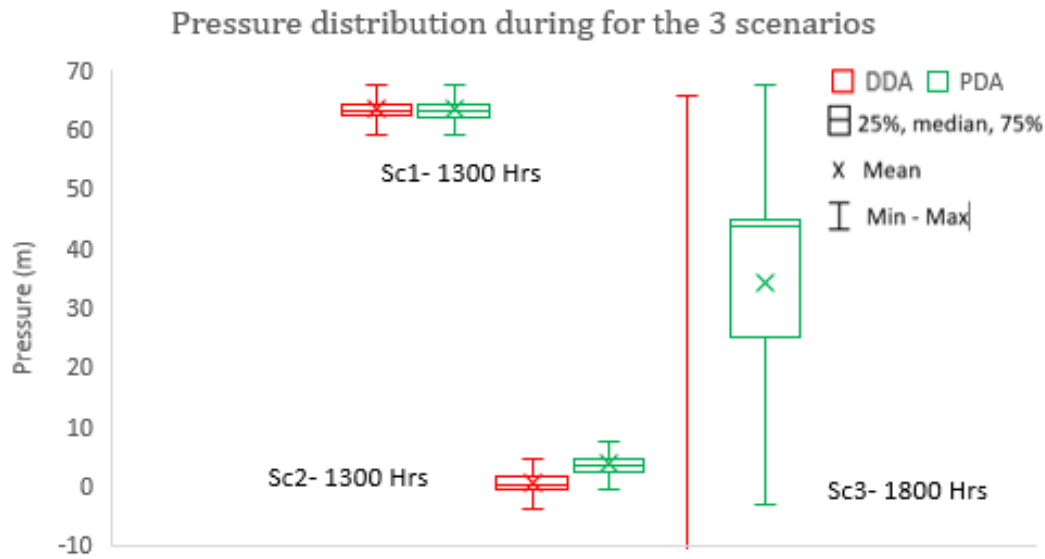


Figure 4.3: Statistical pressure distribution, minimum, median (50<sup>th</sup> percentile), mean, maximum, 25<sup>th</sup> percentile, and 75<sup>th</sup> percentile during peak hour times for scenario 1-3.

### 4.3. Low/Negative pressure zoning

Spatial pressure distributions are presented in Figure 4.4 for low pressure scenarios 2 and 3 for both PDA and DDA. The areas most affected can be observed from the figures marked in color red with pressure below zero. The extent of the affected area is higher while using DDA, Figure 4.4 (a) compared to PDA, Figure 4.4 (b) for scenario 2. A similar trend was observed in scenario 3, with enormous overestimation of the areas with low/ negative pressure using the DDA model as shown in Figure 4.4 (c) in comparison with the PDA model, Figure 4.4 (d).

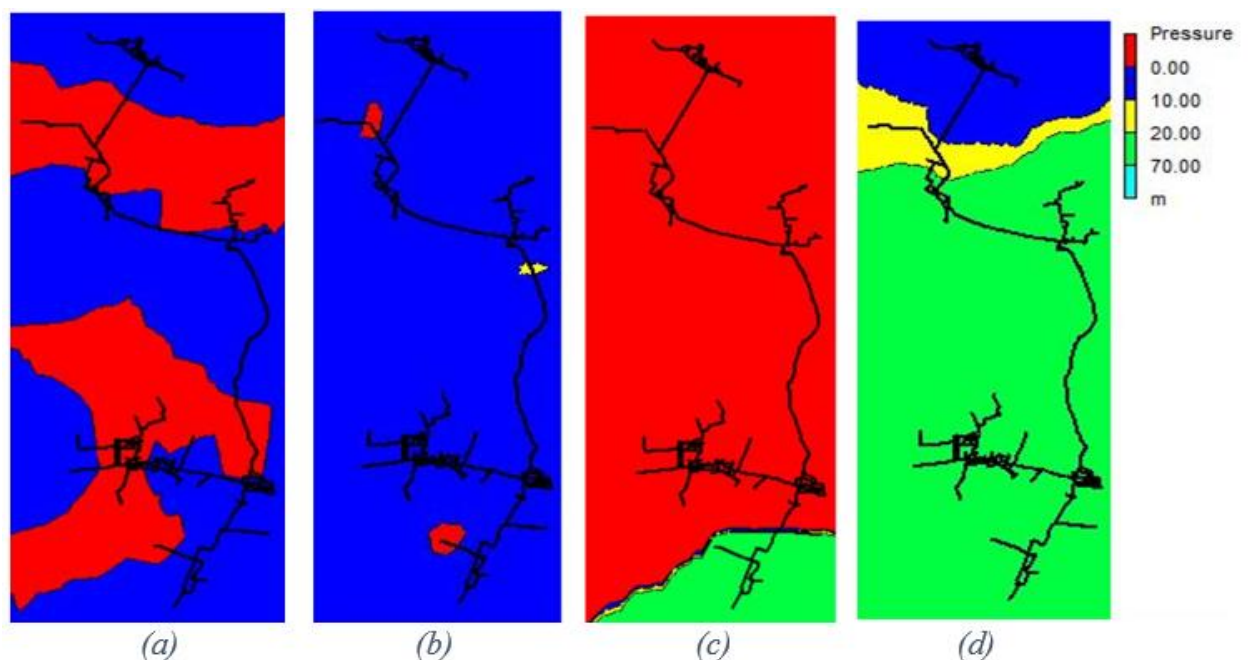


Figure 4.4: Spatial distribution of low/negative pressure for scenario 2 at 13:00 for (a) DDA (b) PDA and scenario 3 at 19:00 for (c) DDA & (d) PDA.

Under sustained low pressure events, the DDA model cannot be relied upon to correctly estimate the areas prone to intrusion of external contaminants and or backflow. Using PDA, the overall nodes considered critical (pressure below 0 and requiring mitigation measures) and those considered susceptible to backflow/intrusion (pressure 0-15 m) are shown in Table 4.2 below.

*Table 4.2: Distribution of nodes with negative pressure using the PDA model.*

Nodes	Scenario 2	Scenario 3
Total number of nodes	1167	1167
Number of nodes with pressure below 0 m (risky)	27	34
Number of nodes with pressure between 0-15 m (susceptible)	1140	919
% Of nodes below 0 m	2.3	2.9
% Of nodes between 0-15 m	97.7	78.7

#### 4.4. Pathogen intrusion rate into the WDN

Unit intrusion rate was influenced by the intrusion head ( $H_{\text{pressure drop}}$ ) and the size of the leakage holes as seen in Table 4.3. Scenario 2 with a high intrusion head and higher leakage area experienced a unit intrusion rate of 0.0042 l/s\*km compared to 0.0039 l/s\*km as seen in scenario 3. The total intrusion rate was subject to the length of the pipeline with leakage as seen in Table 4.3.

*Table 4.3: Resulting intrusion rate,  $Q_{\text{int}}$ , into EPANET used to calculate the intrusion mass flow of pathogens.*

Description	Scenario 2	Scenario 3
$H_{\text{normal}}$ (m)	57.16	63.03
Intrusion Area A ( $\text{mm}^2$ )	1.55	1.48
$H_{\text{pressure drop}}$ (m)	1.0201	0.9730
$Q_{\text{int}}$ Intrusion rate per km (l/s*km)	0.0042	0.0039
Intrusion section (m)	1.5093	0.5413
$Q_{\text{int}}$ - Intrusion rate (l/s)	0.0063	0.0021

By using the concentrations of pathogens in soil water and the intrusion rate presented in table 4.3, the mass flow in number per hour into the WDN was calculated as presented in table 4.4 below.

*Table 4.4: Calculated intrusion mass flow set into EPANET as a mass booster. It is calculated by multiplying the intrusion rate and calculated concentrations of pathogens.*

Pathogen	Concentration [No/L]	Mass flow [No/s]	Mass flow [No/h]
<b>Scenario 2</b>			
Norovirus	1 808	11.37	40 945
Cryptosporidium	348	2.42	8 697
Campylobacter	1 200	75.49	271 773
<b>Scenario 3</b>			
Norovirus	1 808	3.79	13 656

<i>Cryptosporidium</i>	384	0.81	2 901
<i>Campylobacter</i>	1 200	25.18	90 643

#### 4.5. Pathogen distribution in the WDN during sustained low pressure events

The pathogens were injected into the WDN at nodes and distributions using the PDA model were observed when most people were assumed to be consuming the water at 19:00. From spatial distributions figure 4.5, higher concentrations of Pathogens, *Campylobacter* (Figure 4.5 (a-b)), *Cryptosporidium* (Figure 4.5(c-d)), and *Norovirus* (Figure 4.5(e-f)) were observed around the North-Eastern section of the WDN for scenario 2 (Figure 4.5 (a, c & e)), while for scenario 3 (Figure 4.5 (b, d & f)), the higher concentrations can be observed in the North-Western part of the WDN.

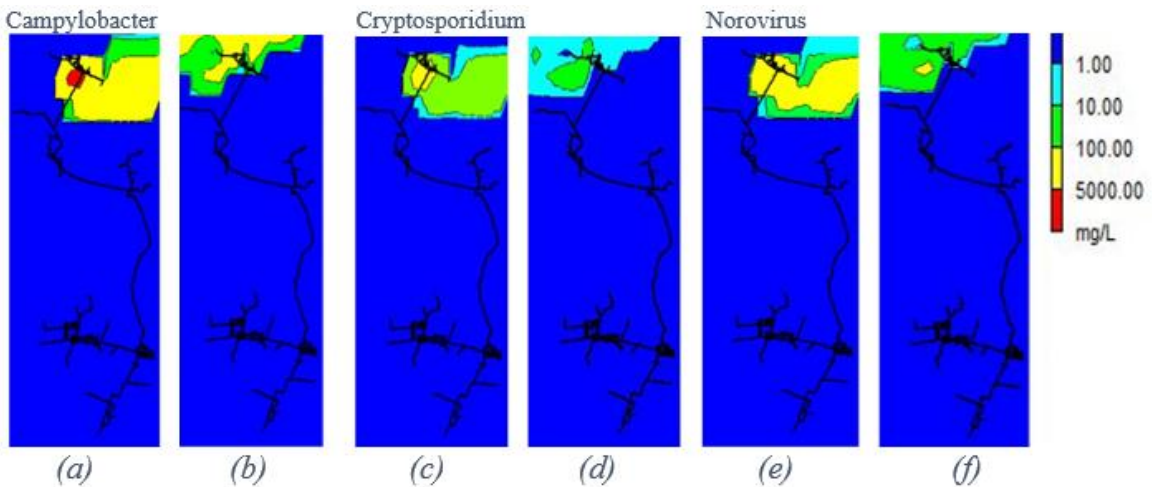


Figure 4.5: Spatial distribution of pathogens (PDA) at 19:00. for *Campylobacter* (a) scenario 2, (b) scenario 3; *Cryptosporidium* (c) scenario 2, (d) scenario 3; and *Norovirus* (e) scenario 2, (f) scenario 3.

Statistical distribution of pathogens (*Campylobacter*, *Cryptosporidium*, and *Norovirus*) concentration across all nodes in the network are displayed in Figures 4.6 – 4.8, for periods 19:00 – 22:00. after low pressure intrusion event for both scenarios 2 and 3. The highest concentrations were observed for scenario 2 compared to the scenario at 19:00 for all three cases.

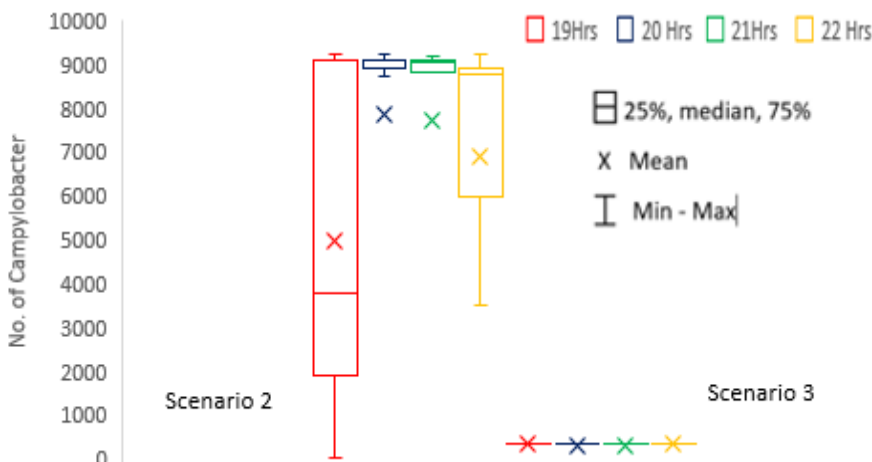


Figure 4.6: Statistical distribution of *Campylobacter* concentrations at 19:00 – 22:00 for scenarios 2 and 3.

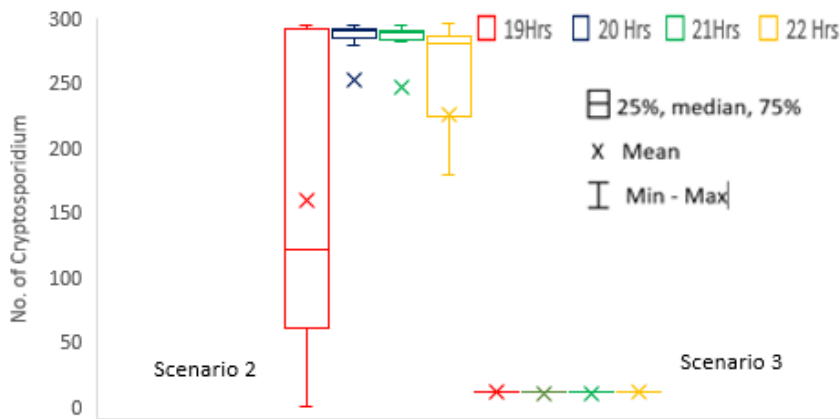


Figure 4.7: Statistical distribution of *Cryptosporidium* concentrations at 19:00 – 22:00 for scenarios 2 and 3.

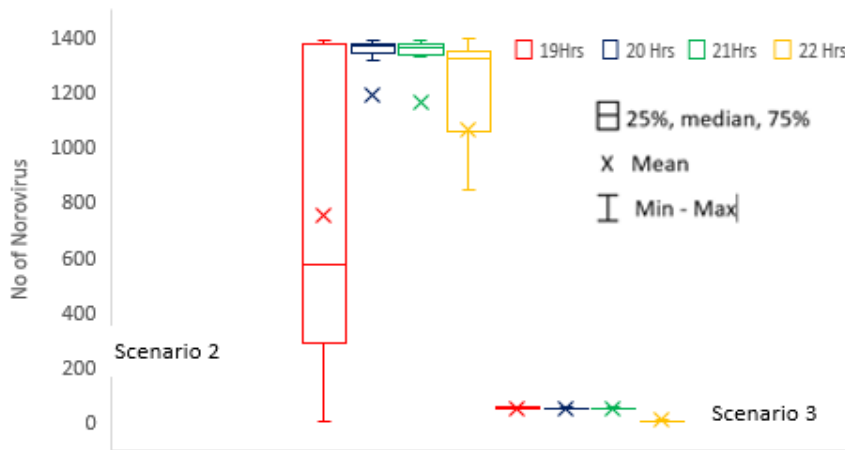


Figure 4.8: Statistical distribution of *Norovirus* concentrations at 19:00 – 22:00 for scenarios 2 and 3.

The highest observed pathogen concentrations, at 19:00 in both scenarios, were used for the analysis of the risks in the QMRA tool. The triangular (T) distributions, (minimum; mode; maximum) values at this hour were determined and are summarized in Table 4.5.

Table 4.5: Modelled concentrations of pathogens (No/L) *Campylobacter*, *Cryptosporidium*, and *Norovirus* at 19:00 generated from EPANET

Pathogen [No/L]	Scenario 2	Scenario 3
<i>Campylobacter</i>	T (0.13; 9 160 <sup>1</sup> ; 9 228) <sup>2</sup>	T (71.8; 345; 397)
<i>Cryptosporidium</i>	T (0.01; 290 <sup>1</sup> ; 295) <sup>2</sup>	T (2.3; 10; 12.7)
<i>Norovirus</i>	T (0.02; 1 370 <sup>1</sup> ; 1 390) <sup>2</sup>	T (10.8; 50; 59.8)

<sup>1</sup> This value is assumed by rounding the values to the nearest five

<sup>2</sup> Distributions: T (min; mode; max)

#### 4.6. Risk analysis in QMRA

As can be seen in Table 4.6 below, none of the pathogens meet the guideline value of  $10^{-6}$  infected per day. Both scenarios lead to a virtually 100 % probability for infection by all the pathogens of the population exposed during the most critical hour (19:00).

Table 4.6: Hourly probability of infection for scenario 2 and 3 presented for 5<sup>th</sup>, 25<sup>th</sup>, 50<sup>th</sup>, 75<sup>th</sup>, and 95<sup>th</sup> percentile for each reference pathogen

<b>P<sub>inf, hourly</sub> 19:00 – Scenario 2</b>			
	<b><i>Campylobacter</i></b>	<b><i>Norovirus</i></b>	<b><i>Cryptosporidium</i></b>
0.05	1.0	0.0	1.2E-009
0.25	1.0	0.0	2.89E-003
0.5	1.0	1.0	1.0
0.75	1.0	1.0	1.0
0.95	1.0	1.0	1.0
<b>P<sub>inf, hourly</sub> 19:00 – Scenario 3</b>			
	<b><i>Campylobacter</i></b>	<b><i>Norovirus</i></b>	<b><i>Cryptosporidium</i></b>
0.05	0.0	0.0	3.92E-011
0.25	7.99E-004	0.0	6.25E-005
0.5	1.0	1.0	0.038
0.75	1.0	1.0	1.0
0.95	1.0	1.0	1.0

## 5. Discussion

The potential for contamination of drinking water in water distribution networks (WDN) through pathogen intrusion due to low pressure events has been studied in different studies across the world as discussed in Chapter 2. The studies, utilizing hydraulic modeling and field assessments, have proposed a framework suitable for assessing the health risks resulting from the intrusions (Hatam et al., 2018). In WDNs, common adverse pressure events occur as prolonged low-pressure events or transient events. These events, based on evidence from modeling and field data can last for a short duration such as milliseconds to prolonged periods such as minutes, hours, and days (Hatam et al., 2018). It is anticipated the frequency of the intrusion events is more likely to increase due to the aging of WDN infrastructure. Characterizing the WDN infrastructure based on spatial distribution, intensity, and duration of adverse pressure events is thus necessary for the protection of public health.

### 5.1. Hydraulic modeling under sustained low pressure conditions

Using the demand-driven analysis (DDA) model assumes fixed parameters for demand flow in nodes for the continuity equation used in EPANET. Satisfying these demands under low pressure events may result in values of pressure that are unrealistic. Pressure driven analysis (PDA) model fixes this inability by estimating demand at the nodes (junctions) based on the available pressure at the nodes (Hatam et al., 2018).

For scenarios 2 and 3 with low demand satisfaction of 32.5 % and 33.4 % respectively, significant differences in nodal pressures between the DDA and PDA were observed compared to scenario 1 with 100 % demand satisfaction ( Figure 4.3). These observations indicate the unreliability of the DDA as a tool for modeling low pressure conditions. Utility managers ought to adopt a PDA model for the identification of critical areas in WDN susceptible to pathogen intrusion from low pressure occurrences.

DDA underestimated pressure not only at nodes experiencing low pressures below 13 m, as seen from PDA, but it also included nodal pressures as high as 60m, though, smaller variations were commonly seen for relatively high nodal pressure. The extents in the pressure difference were also influenced by low pressure conditions' severity. However, no limiting pressure in the tested pressure range, less than 78.8 m, was detected above which the two models would experience convergency for all nodes and in all study cases (scenarios). The variations in pressure at the nodes have a direct impact on the delineation of areas in the WDN that are vulnerable to intrusion and backflow.

### 5.2. Spatial distribution of zones vulnerable to intrusion

Identification of zones vulnerable to pathogen/contamination intrusion depends on the identification of zones vulnerable to low pressure events. The zones are generally defined by considering minimum pressure which when exceeded would result in backflow or intrusion (Hatam et al., 2018). Different regions and countries have different guidelines for setting minimum positive pressures. According to Hatam et al, (2018), if pressure drops below 14 m in the event of a WDN main pipeline break, it is common for utilities to issue boil water advisories (BWA).

Nodes experiencing pressure below 0 m are considered to have a higher risk of intrusion hence justifying the BWA. Nodes with pressure between 0 and 15 m can be considered

susceptible to intrusions hence recommendations for mitigation measures in the WDN is necessary (Hatam et al., 2018).

For the studied water distribution network, the minimum pressure criteria used was 0 m. For scenario 2, 27 nodes were identified as risky (necessary for issuance of BWA) and 1,140 nodes were deemed susceptible to backflow/intrusion while 34 and 919 nodes were identified as risky and susceptible respectively for scenario 3. A small number of risky nodes can lead to high public health impact depending on contaminant concentrations, rates of intrusion and the level of vulnerability of the population served (Hatam et al., 2018). Minimal pressure criterion is necessary when specifying the extent of vulnerable areas however real-time online monitoring should be used to trigger an actual response.

For scenarios 2 and 3, the PDA model significantly reduces the negative pressure zones in the WDN (Figure 4.4 (b) and (d)). Similarly, clustering is necessary for the determination of BWA zone boundaries (Figure 4.4). The extent of the BWA zone depends on the pressure criteria chosen and increasing the minimal pressure criteria will increase the affected area.

Other than the use of PDA-based hydraulic modeling other factors that utility managers should consider before issuing a BWA include low pressure event durations, real-time monitoring data from sensors, vulnerable users of the WDN (such as hospitals, elderly homes, daycare centers, and hospitals) disinfectant residuals at the onset of pressure drop, the number of high-rise buildings in risky zone, availability of backflow control devices and area zoning depending on use, such as industrial use (Hatam et al., 2018).

### **5.3. Contaminant intrusion**

The driving force for intrusion is the pressure differential in and out of the WDN pipe. Maintaining high internal pressure compared to external pressure limits the intrusion (Yang et al., 2011).

Unit intrusion rate was influenced by the intrusion head ( $\Delta H_{\text{pressure drop}}$ , which is the difference between the inside and outside of the hole in the pipe when the pump is shut off) and the size of the leakage holes. In Table 4.3, scenario 2 indicates a high intrusion head and higher leakage area and a subsequent high unit intrusion rate of 0.0042 l/s\*km compared to 0.0039 l/s\*km seen in scenario 3. The total intrusion rate was subject to the length of the pipeline with leakage as seen in Table 4.3. Scenario 2 had approximately 1.5 km of pipeline within the negative pressure (risky) zone this contributed to an intrusion of 0.0063 l/s while 0.0021 l/s was observed for scenario 3 with a total of 0.54 km. The duration of the low pressure event had a higher impact on pathogen intrusion as it influenced the number of pathogens intruding into the system as well as the probability of water consumption coinciding with the availability of pathogens at the consumption node. Longer durations meant more users of the WDN were likely to consume the supplied water.

In the simulations, it was assumed that all the water around the pipes in the low pressure zone was contaminated by pathogens and that the concentration was the same everywhere, which may not be a correct assumption. This was a possible source for an overestimation of the pathogen intrusion.

The assumption that there is a ratio between E. coli and the pathogens, as well as that the ratio would be the same for wastewater and soil water introduces a significant level of

uncertainty. It is known that the persistence of pathogens depends on pH, temperature, and other environmental factors as well as that the survival in water differs. Since the analysis relies on the estimated maximum values it is reasonable to believe that the result is not underestimating the risk but rather overestimating.

#### **5.4. Water Quality-Fate and transport of pathogens**

EPANET 2.2 water quality modeling tool was applied to model the fate and transportation of pathogens in the WDN. This is a single species model that was used for tracking the movement and fate of one species at a time. The species were assumed to be non-reactive. Interaction of pathogen with disinfectant residuals, such as chlorine, and with biofilms was not considered in this simulation. Worst-case scenarios were assumed where the inactivation of pathogens was not taken into account. Other than *Cryptosporidium* which is more resistant to chlorine inactivation, other pathogens used, *Campylobacter* and *Norovirus*, can have log reductions in the presence of residual disinfectant (Besner et al., 2011).

For water quality modeling, extended period simulation (EPS) was used to model pathogens' fate and transportation beginning at the entry point into the WDN to the consumption nodes for the estimation of consumers exposed to pathogens due to associated low pressure events. The event start time, the intrusion nodes, number of pathogens intruding the WDN per hour (mass rate), and duration of the event were used as inputs to the simulation.

The concentration of pathogens at 19:00 for the consumer nodes with a concentration greater than zero was used for the determination of the risks of infection using the QMRA tool. Higher values were observed in scenario 2 compared to scenario 3, this was due to the longer intrusion duration and greater section experiencing negative pressure compared to high average negative pressure, and bigger leak orifice compared to scenario 3.

Concentration values were picked at 19: 00 since it was determined as the hour where the risk to human health was the most. In the study by Hatam et al, (2019) over 2 days, the probability of consumers drinking water at this time ranged from 70% to 100%.

#### **5.5. Health risk characterization (QMRA)**

The application of Analytica for QMRA in this study was different from most applications where the impact of barriers on raw water to provide safe drinking water was studied. Instead, it was investigated how highly contaminated water due to a sudden strong intrusion will infect the population exposed.

The result from QMRA in this report confirms the certainty for infection of the exposed population which is also expected to occur from these kinds of events. The event was a worst-case scenario with a duration of up to five hours, but a low probability for occurrence. It relies on a chain of events to occur simultaneously where each of these events has or may have a low probability.

Firstly, the pump failure causing the head drop like this is a very rare event. Secondly, a scenario where the need to engage three fire hydrants as modeled simultaneously is also very unlikely. Both of these events can be prepared, and their impact can be mitigated

through shutting off the water supply to the consumers that would be exposed and through additional flushing.

It is also worth commenting that in calculating input values into the EPANET, pathogen levels chosen were the maximum from literature meaning that the most probable level is lower, which may further reduce the overall infection risk.

## **5.6. Mitigation measures**

To minimize the impact on public health from intrusions due to sustained low pressure conditions utilities must put in place measures for mitigating risks. Yang et al,(2011) suggest exposure reduction and reduction of pathogen concentrations in WDN demand nodes as the primary measures for reducing risks. Risk reduction measures include management of pressure in the WDN, implementing leak detection and repair programs, and ensuring a safe spacing of pipe conveying drinking water from the sewer pipe. Maintaining disinfectant residuals was the main way of reducing the concentration of pathogens at the demand nodes (Yang et al., 2011). For this project site, negative pressure events were observed to be the main cause of intrusions in the presence of leaks hence the biggest contributor to human health risks. Maintaining required pressures can be considered cheaper and easier to manage options compared to other practices such as leak repairs. Planning for decontamination in low pressure zones is thus necessary in case of contamination events. Online monitoring devices such as sensors can be used to provide real-time data on pressure and quality changes to guide timely interventions.

## 6. Conclusions and recommendations

This section highlights the conclusions of the study and recommendations to the water utilities.

### 6.1. Conclusions

Hydraulic simulations using EPANET 2.2 were conducted for a WDN under various sustained low pressure conditions and the results were compared to operations under normal working conditions. Scenarios on pump failure in the WDN and sudden change in demand due to emergency fire water supply were used to simulate the low pressure conditions. The critical pressure value of 0m, necessary to trigger intrusion, was used in this study. The pressure value varies in different regions/countries and depending on specific site conditions. The number of nodes in the WDN requiring remediation measures was identified and zoning of the critical low pressure areas was identified. Overall, 27 nodes were critically affected in the case of the pump failure, scenario2, representing 2.3% of the total nodes. During a fire emergency, scenario 3, 37 nodes were identified accounting for 2.9% of all nodes.

Simulations were done with both the DDA and PDA models and the results indicated high underestimation of pressure by the DDA model resulting in a larger area with critical pressure. This pressure underestimation by the DDA could lead to unnecessary BWA by water utilities, hence it is not recommended for use in such situations, instead, PDA pressure models should be used that can give realistic pressure in low pressure situations.

Using the orifice equation, delineated zones under negative pressure, negative pressures on nodes, intrusion volume rates through the system were determined as 0.0063 and 0.0021 L/s for scenarios 2 and 3, respectively. Using the concentration in soil water, the pathogen mass rate into the system was determined. Hydraulic/water quality model was used to determine pathogen numbers at any specific place node at a specific time and used for risk characterization using the QMRA tool.

The results from the QMRA were expected to not meet the guidelines. It is concluded that both events have a low probability to happen but if it does, the risk of infection for the consumer exposed is 100%. It was also concluded that the results may be an overestimation since the input values represented the maximum pathogen levels as well as that the chosen concentration of *E.coli* in soil water measured in Gothenburg was the highest value. Another factor for the high concentrations is that all pipes where intrusion was expected to occur were assumed to have contaminated water around them.

### 6.2. Recommendations

To reduce the risk of infection to consumers proactive strategies must be adopted by the water utilities. Monitoring of water quality in WDN is one such strategy. This strategy depends on the strategic selection of appropriate monitoring sites. A risk-based analysis tool combined with GIS can be necessary for prioritizing pipe sections for water quality monitoring. The tool should be able to analyze the physical and hydraulic integrity of the WDNs such as pipe age and materials; contamination threats such as contaminant sources; and vulnerable consumers such as hospitals, elderly homes, and daycares. Through WDN network analysis and mapping sensitive areas, a better-quality management strategy can be adopted.

In the study, critical areas were identified based on pressure criteria selected and EPANET Contour mapping was used to display the data. The risks were estimated using the QMRA tool. However, the hydraulic/water quality modeling tool used was only capable of a single objective analysis. Utilities thus ought to adopt tools capable of multiple objective analysis. Water network management (Aquis) tool is recommended, in this system, WDN characterization based on hydraulic, quality, physical, and operational parameters is possible. GIS data, real-time data from SCADA, as well weather data can be incorporated into the system to provide realistic risk estimation. Other tools include Mike Urban+ which is capable of analysis involving the entire WDN or part of it under various hydraulic conditions such as steady-state analysis, extended period simulation, and analysis due to water hammer situations. Water quality analysis can be incorporated in any of the conditions when necessary.

## 7. Further studies

EPANET 2.2 water quality model used is a single species model that can be used for tracking the movement and fate of one species at a time. This results in an overestimation of the risks as necessary interactions, that can impact pathogen concentrations, are not analyzed. Similarly, the model assumes only advective transport while in real fluid flow longitudinal dispersion occurs. The upgraded model, EPANET MSX can help achieve realistic values and is thus recommended for use in further studies. The model is capable of simulating fate and transport involving various dissolved or suspended substances in a WDN in bulk fluid flow and at the pipe walls. The model has the additional capability to model multiple species unlike in other EPANET versions (Seyoum & Tanyimboh, 2017). It can model the interactions between different species in the bulk flow as well as in the pipe walls by providing solutions to a set of “differential-algebraic equations (DAEs)” provided by the user (Hatam et al., 2018).

To further estimate the health risk, it would be preferred to take water samples in the catchment area to measure *E.coli* in soil water in different locations along the distribution network and simulate both minimum and maximum levels. It would also be preferred to analyze varying levels of pathogens in the soil water to find which levels may be critical for this system.

The most likely effective mechanism for human health risk mitigation is reducing the risk of exposure (Yang et al., 2011). This reduces the chances of consumers being exposed to contaminated water during consumption. Highly infectious pathogens can cause infection even with a single pathogen for instance virus such as *Norovirus* (Yang et al., 2011). The oocysts, such as *Cryptosporidium*, on the other, are resistant to inactivation by residual disinfectant hence inactivation, as a control mechanism, for this type of pathogens might not reduce infection risks (Besner et al., 2011). As observed in the simulations during the study, the pathogens’ residence time in the WDN is lower hence conventional quality control measures such as testing at the end-user nodes might not detect the contamination in time. Exposure reduction measures, such as pressure and water quality management in the case of the project area, can go a long way in reducing the risk of infection to human health.

Online monitoring of pressure and quality using sensors can help identify pressure deficient situations as well as exact locations for quality breaches and in turn act as an early warning system in the event of intrusion. The current study limitations include concentrating intrusions over an affected section at a single node with the lowest pressure, which is not realistically the case. Similarly, the EPANET tool used has also shown insufficiencies in intrusion tracking with respect to time (Sami, 2018). User inputs guide the time patterns which influence the response outputs however contaminant source tracking requires time-variant calculations (Sami, 2018). With sensors, it is possible to overcome the limitations and hence provide information that can guide preventive measures, including issuing of BWA, well in advance for risk reduction. Sensor optimization is possible with data from the EPANET such as flow parameters and zoning of concentration areas with the aid of contour mapping to obtain the best locations for sensors. Additionally, it is possible to minimize detection times and data storage space using sensor response data simulation algorithms (Sami, 2018). Human health risk can be greatly reduced with the use of real-time data provided by sensors and thus highly recommended for use in a WDN.



## 8. References

- Arvidsson, D. (2019). *Utredning av avloppsprocessers påverkan på recipientens mikrobiologiska status*.
- Aspevall, O., Carlin, K., Hedlund, K. O., Struwe, O., & Zetterqvist, I. (2014). *Vinterkräksjuka i vården : kunskapsunderlag för att minska spridningen av norovirus*.
- Ballester, F., & Sunyer, J. (2000). Drinking water and gastrointestinal disease: Need of better understanding and an improvement in public health surveillance. *Journal of Epidemiology and Community Health*, 54(1), 3–5. <https://doi.org/10.1136/jech.54.1.3>
- Besner, M. C., Prévost, M., & Regli, S. (2011). Assessing the public health risk of microbial intrusion events in distribution systems: Conceptual model, available data, and challenges. *Water Research*, 45(3), 961–979. <https://doi.org/10.1016/j.watres.2010.10.035>
- Bjelkmar, P., Hansen, A., Schönning, C., Bergström, J., Löfdahl, M., Lebbad, M., Wallensten, A., Allestam, G., Stenmark, S., & Lindh, J. (2017). Early outbreak detection by linking health advice line calls to water distribution areas retrospectively demonstrated in a large waterborne outbreak of cryptosporidiosis in Sweden. *BMC Public Health*, 17(1). <https://doi.org/10.1186/s12889-017-4233-8>
- Blokker, M., Agudelo-vera, C., Moerman, A., van Thienen, P., & Pieterse-Quirijns, I. (2017). Review of applications of SIMDEUM, a stochastic drinking water demand model with small temporal and spatial scale. *Drinking Water Engineering and Science Discussions*, 1–15. <https://doi.org/10.5194/dwes-2017-4>
- Blokker, M., Smeets, P., & Medema, G. (2014). QMRA in the drinking water distribution system. *Procedia Engineering*, 89, 151–159. <https://doi.org/10.1016/j.proeng.2014.11.171>
- Blokker, M., Smeets, P., & Medema, G. (2018). Quantitative microbial risk assessment of repairs of the drinking water distribution system. *Microbial Risk Analysis*, 8(December 2017), 22–31. <https://doi.org/10.1016/j.mran.2017.12.002>
- CDC. (2009). *Drinking Water Treatment Methods for Backcountry and Travel Use*.
- CDC. (2014). *Questions and Answers | E. coli | CDC*.
- CTI resources. (2021). *Aquis Water Network Management Software | CTI Resources*. <https://www.ctiresources.com.my/product/water-network-management-aquis/>
- Davis, M. J., Janke, R., & Magnuson, M. L. (2014). A framework for estimating the adverse health effects of contamination events in water distribution systems and its application. *Risk Analysis*, 34(3), 498–513. <https://doi.org/10.1111/risa.12107>
- DHI Water & Environmental, . (2011). *Mike urban water distribution*.
- Dienus, O., Sokolova, E., Nyström, F., Matussek, A., Löfgren, S., Blom, L., Pettersson, T. J. R., & Lindgren, P. E. (2016). Norovirus Dynamics in Wastewater Discharges and in the Recipient Drinking Water Source: Long-Term Monitoring and Hydrodynamic Modeling. *Environmental Science and Technology*, 50(20), 10851–10858. <https://doi.org/10.1021/acs.est.6b02110>
- Gibbs, S. G., Meckes, M. C., & Scarpino, P. V. (2003). The effect of long-term wastewater cross-connection on the biofilm of a simulated water distribution system. *Journal of Environmental Engineering and Science*, 2(2), 85–98. <https://doi.org/10.1139/s03-005>
- Hassan, E., & Baldrige, M. T. (2019). Norovirus encounters in the gut: multifaceted interactions and disease outcomes. *Mucosal Immunology*, 12(6), 1259–1267. <https://doi.org/10.1038/s41385-019-0199-4>
- Hatam, F., Besner, M.-C., Ebacher, G., & Prévost, M. (2018). Combining a Multispecies

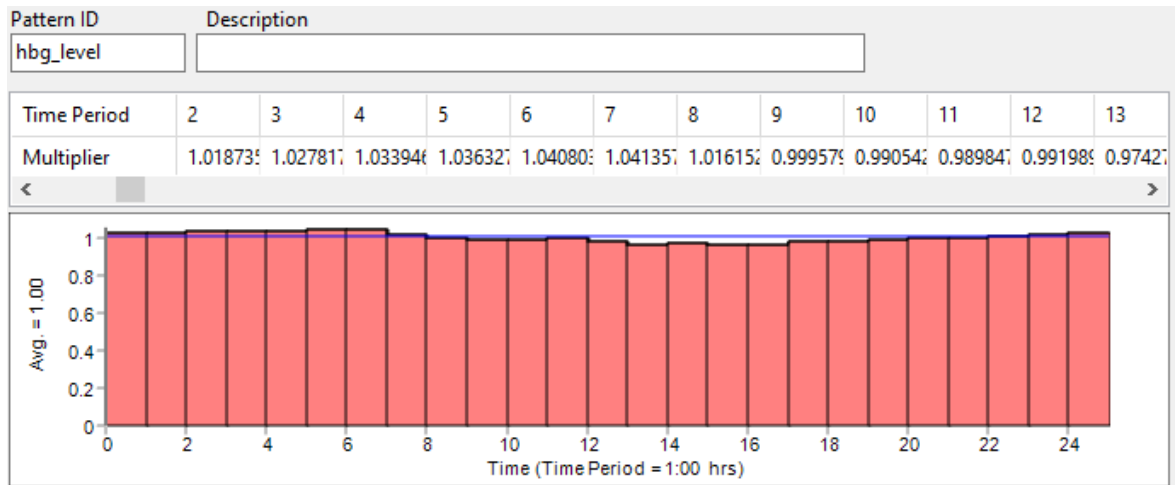
- Water Quality and Pressure-Driven Hydraulic Analysis to Determine Areas at Risk During Sustained Pressure-Deficient Conditions in a Distribution System. *Journal of Water Resources Planning and Management*, 144(9), 04018057. [https://doi.org/10.1061/\(asce\)wr.1943-5452.0000976](https://doi.org/10.1061/(asce)wr.1943-5452.0000976)
- Hatam, F., Blokker, M., Besner, M. C., Ebacher, G., & Prévost, M. (2019). Using nodal infection risks to guide interventions following accidental intrusion due to sustained low pressure events in a drinking water distribution system. *Water (Switzerland)*, 11(7). <https://doi.org/10.3390/w11071372>
- Havelaar, A. H., De Hollander, A. E. M., Teunis, P. F. M., Evers, E. G., Van Kranen, H. J., Versteegh, J. F. M., Van Koten, J. E. M., & Slob, W. (2000). Balancing the risks and benefits of drinking water disinfection: Disability adjusted life-years on the scale. *Environmental Health Perspectives*, 108(4), 315–321. <https://doi.org/10.1289/ehp.00108315>
- Henze, M. H., Harremoës, P., Jansen, J. la C., & Arvin, E. (2002). *Wastewater Treatment: Biological and Chemical Processes* (3rd ed.).
- Islam, N., Sadiq, R., & Rodriguez, M. J. (2017). Optimizing Locations for Chlorine Booster Stations in Small Water Distribution Networks. *Journal of Water Resources Planning and Management*, 143(7), 04017021. [https://doi.org/10.1061/\(asce\)wr.1943-5452.0000759](https://doi.org/10.1061/(asce)wr.1943-5452.0000759)
- Lalancette, C., Papineau, I., Payment, P., Dorner, S., Servais, P., Barbeau, B., Di Giovanni, G. D., & Prévost, M. (2014). Changes in Escherichia coli to Cryptosporidium ratios for various fecal pollution sources and drinking water intakes. *Water Research*, 55, 150–161. <https://doi.org/10.1016/j.watres.2014.01.050>
- Larsen, S. L., Christensen, S. C. B., Albrechtsen, H.-J., & Rygaard, M. (2017). GISMOWA: Geospatial Risk-Based Analysis Identifying Water Quality Monitoring Sites in Distribution Systems. *Journal of Water Resources Planning and Management*, 143(6), 04017018. [https://doi.org/10.1061/\(asce\)wr.1943-5452.0000754](https://doi.org/10.1061/(asce)wr.1943-5452.0000754)
- Mandel, P., Maurel, M., & Chenu, D. (2015). Better understanding of water quality evolution in water distribution networks using data clustering. *Water Research*, 87, 69–78. <https://doi.org/10.1016/j.watres.2015.08.061>
- McInnis, D. (2004). A relative-risk framework for evaluating transient pathogen intrusion in distribution systems. *Urban Water Journal*, 1(2), 113–127. <https://doi.org/10.1080/15730620412331290010>
- Mena, K. D., Mota, L. C., Meckes, M. C., Green, C. F., Hurd, W. W., & Gibbs, S. G. (2008). Quantitative microbial risk assessment of a drinking water – wastewater cross-connection simulation. *Journal of Environmental Engineering and Science*, 7(5), 525–530. <https://doi.org/10.1139/S08-022>
- Nyende-Byakika, S., Ngirane-Katashaya, G., & Ndambuki, J. M. (2013). Application of hydraulic modelling to control intrusion into potable water pipelines. *Urban Water Journal*. <https://doi.org/10.1080/1573062X.2012.699072>
- Ostfeld, A., Kessler, A., & Goldberg, I. (2004). A contaminant detection system for early warning in water distribution networks. *Engineering Optimization*, 36(5), 525–538. <https://doi.org/10.1080/03052150410001714097>
- Paneth, N., Vinten-Jahansen, P., Brody, H., & Rip, M. (1998). A Rivalry of foulness: official and unofficial investigations of the London cholera epidemic of 1854. *American Journal of Public Health*, 88(10), 1545–1553.
- Petterson, S. R., & Ashbolt, N. J. (2016). QMRA and water safety management: Review of application in drinking water systems. *Journal of Water and Health*, 14(4), 571–589. <https://doi.org/10.2166/wh.2016.262>

- Pettersson, T., Madeleine, F., Åström, J., Pott, B.-M., & Almqvist, H. (2017). *Vidareutveckling av QMRA-verktyget-fas 1*.
- Rathi, S., & Gupta, R. (2017). Optimal sensor locations for contamination detection in pressure-deficient water distribution networks using genetic algorithm. *Urban Water Journal*. <https://doi.org/10.1080/1573062X.2015.1080736>
- Rikard Dryselius, J. T. M. S.-S. A. M. (2013). *Mikrobiologiska risker vid dricksvattendistribution*.
- Rossmann, L. A., Woo, H., Tryby, M., Shang, F., Janke, R., & Haxton, T. (2020). Epanet 2.2 User 's Manual. In *National Risk Management Research Laboratory Office of Research and Development. U.S. Environmental Protection Agency Cincinnati*. <https://www.epa.gov/water-research/epanet>
- Rudrappa, S., & Zharkalli, A. (2018). *Microbial risk assessment of potential pathogen intrusion during planned maintenance work of drinking water distribution system in Gothenburg, Sweden*.
- Sami, M. I. (2018). *Effective placement of sensors for efficient early warning system in water distribution network. September 2018*.
- Säve-Söderbergh, M., Bylund, J., Malm, A., Simonsson, M., & Toljander, J. (2017). Gastrointestinal illness linked to incidents in drinking water distribution networks in Sweden. *Water Research*, 122, 503–511. <https://doi.org/10.1016/j.watres.2017.06.013>
- Schneider Electric. (2021). *Aquis | Schneider Electric Sweden*. <https://www.se.com/se/sv/product-range-presentation/61612-aquis/>
- Schönning, C., Anette, H., Görel, A., Margareta, L., & Lebbad, M. (2011). *Cryptosporidium i Östersund*. In *Smittskyddsinstitutet*.
- Seyoum, A. G., & Tanyimboh, T. T. (2017). Integration of Hydraulic and Water Quality Modelling in Distribution Networks: EPANET-PMX. *Water Resources Management*. <https://doi.org/10.1007/s11269-017-1760-0>
- Sharp, J. H., Clements, K., Diggins, M., McDonald, J. E., Malham, S. K., & Jones, D. L. (2021). E. coli Is a Poor End-Product Criterion for Assessing the General Microbial Risk Posed From Consuming Norovirus Contaminated Shellfish. *Frontiers in Microbiology*, 12(February), 1–14. <https://doi.org/10.3389/fmicb.2021.608888>
- Simões, J., & Dong, T. (2018). Continuous and real-time detection of drinking-water pathogens with a low-cost fluorescent optofluidic sensor. *Sensors (Switzerland)*, 18(7). <https://doi.org/10.3390/s18072210>
- Storey, M. V, Ashbolt, N. J., & Stenström, T. A. (2004). *Biofilms, thermophilic amoebae and Legionella pneumophila – a quantitative risk assessment for distributed water*. 77–82.
- Swedish Civil Contingencies Agency. (2021). *Dricksvattenförsörjning - Krisinformation.se*. <https://www.krisinformation.se/detta-gor-samhallet/mer-om-sveriges-krisanteringssystem/samhallets-ansvar/kommuner/dricksvattenforsorjning>
- Swedish Food Agency, Swedish Public Health Agency, & Swedish Water. (2017). *Cryptosporidium och Giardia* –. 1–9.
- Swedish Institute for Infectious Disease Control. (2011). *Giardia och Cryptosporidium i svenska ytvattentäkter. Svenskt Vatten, SUV Rapport*.
- Swedish Public Health Agency. (2018). *Virus i vatten – metoder för detektion av norovirus*.
- Swedish Water. (2015). *Bedömning av hälsorisker på ledningsnätet vid läcklagning*.
- Taghia, J. (2014). *Bayesian Modeling of Directional Data with Acoustic and Other Applications*.
- Tchobanoglous, G. (1991). *Wastewater engineering : treatment, disposal, and reuse* (3rd

- ed.).
- Teunis, P. F. M., Xu, M., Fleming, K. K., Yang, J., Moe, C. L., & Lechevallier, M. W. (2010). Enteric virus infection risk from intrusion of sewage into a drinking water distribution network. *Environmental Science and Technology*, *44*(22), 8561–8566. <https://doi.org/10.1021/es101266k>
- Tian, P., Yang, D., Shan, L., Wang, D., Li, Q., Gorski, L., Lee, B. G., Quiñones, B., & Cooley, M. B. (2017). Concurrent detection of human norovirus and bacterial pathogens in water samples from an agricultural region in central California Coast. *Frontiers in Microbiology*, *8*(AUG), 1–11. <https://doi.org/10.3389/fmicb.2017.01560>
- van Lieverloo, J. H. M., Mirjam Blokker, E. J., & Medema, G. (2007). Quantitative microbial risk assessment of distributed drinking water using faecal indicator incidence and concentrations. *Journal of Water and Health*, *5*(SUPPL. 1), 131–149. <https://doi.org/10.2166/wh.2007.134>
- Victor, C. P., Ellis, K., Lamar, F., & Leon, J. S. (2021). Agricultural Detection of Norovirus and Hepatitis A Using Fecal Indicators: A Systematic Review. *International Journal of Microbiology*, 2021. <https://doi.org/10.1155/2021/6631920>
- Viñas, V., Malm, A., & Pettersson, T. J. R. (2019). Overview of microbial risks in water distribution networks and their health consequences: Quantification, modelling, trends, and future implications. In *Canadian Journal of Civil Engineering*. <https://doi.org/10.1139/cjce-2018-0216>
- Wéber, R., Huzsvár, T., & Hős, C. (2020). Vulnerability analysis of water distribution networks to accidental pipe burst. *Water Research*, *184*. <https://doi.org/10.1016/j.watres.2020.116178>
- WHO. (n.d.). *Disability weights, discounting and age weighting of DALYs*. Retrieved March 8, 2021, from [https://www.who.int/healthinfo/global\\_burden\\_disease/daly\\_disability\\_weight/en/](https://www.who.int/healthinfo/global_burden_disease/daly_disability_weight/en/)
- WHO. (2003). *ICF checklist: International classification of functioning, disability and health*. <https://www.who.int/classifications/icf/icfchecklist.pdf>
- WHO. (2014). *WHO International Scheme to Evaluate Household Water Treatment Technologies Harmonized Testing Protocol: Technology Non-Specific* (Issue 2015).
- WHO. (2016). *Quantitative Microbial Risk Assessment: Application for Water Safety Management*. World Health Organization. <https://apps.who.int/iris/handle/10665/246195>
- WHO. (2017). *Guidelines for Drinking-Water Quality: Fourth Edition Incorporating the First Addendum*.
- WHO. (2020). Sustainable Development Goals: Guidelines for the Use of the SDG Logo. *United Nations Department of Global Communications*, May.
- Yang, LeChevallier, M. W., Teunis, P. F. M., & Xu, M. (2011). Managing risks from virus intrusion into water distribution systems due to pressure transients. *Journal of Water and Health*, *9*(2), 291–305. <https://doi.org/10.2166/wh.2011.102>
- Yang, Schneider, O. D., Jjemba, P. K., & Lechevallier, M. W. (2015). Microbial risk modeling for main breaks. *Journal - American Water Works Association*, *107*(2), E97–E108. <https://doi.org/10.5942/jawwa.2015.107.0010>
- Yang, Y., Zhu, D. Z., Zhang, T., Liu, W., & Guo, S. (2016). Improved Model for Contaminant Intrusion Induced by Negative Pressure Events in Water Distribution Systems. *Journal of Hydraulic Engineering*, *142*(10), 06016012. [https://doi.org/10.1061/\(asce\)hy.1943-7900.0001176](https://doi.org/10.1061/(asce)hy.1943-7900.0001176)

## 9. APPENDICES

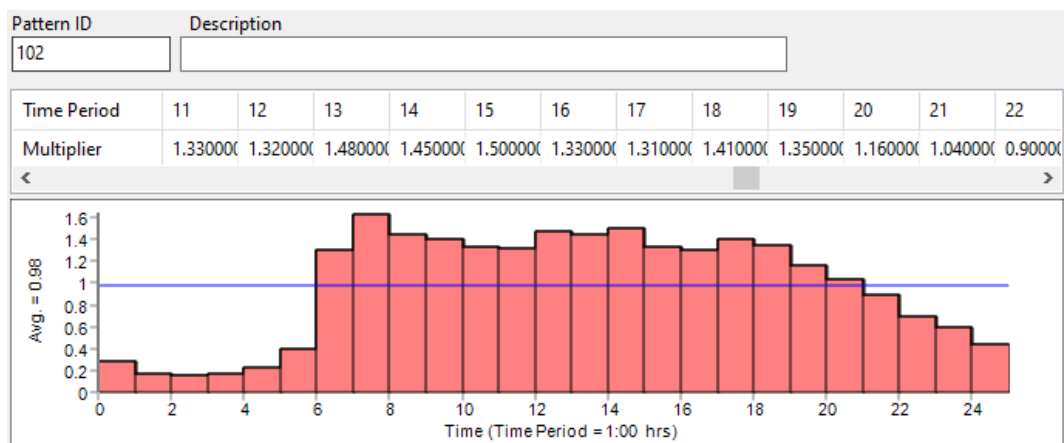
### Appendix 1: Pattern for head distribution (hbg\_level)



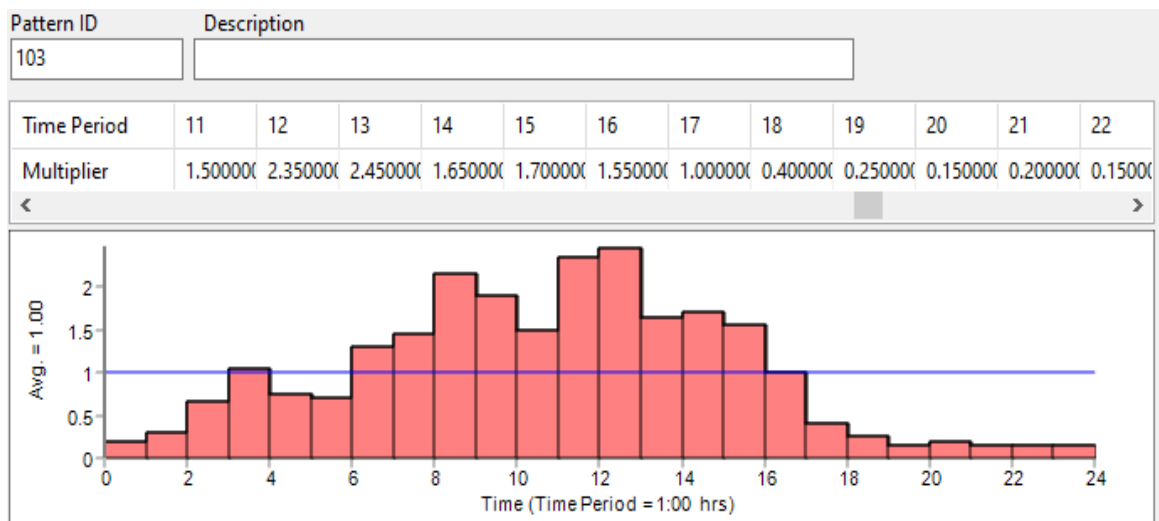
### Appendix 2: Pattern NRW



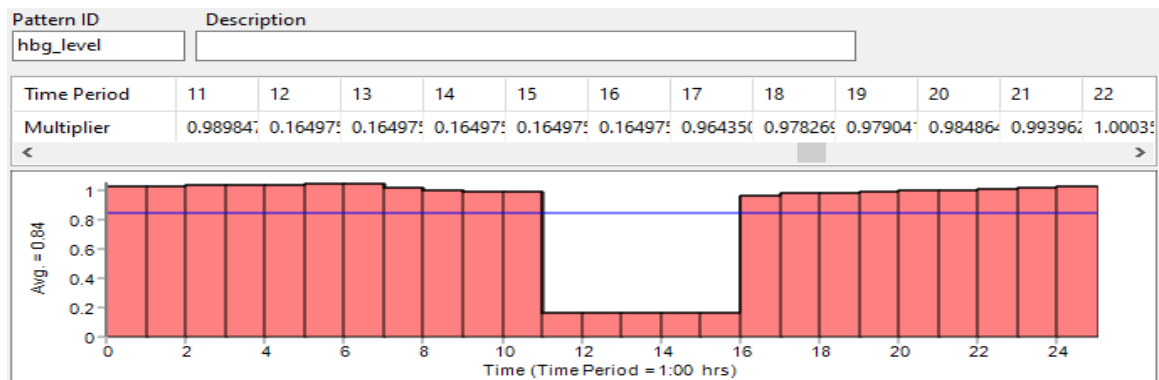
### Appendix 3: Pattern 102 detached and Apartment Housing



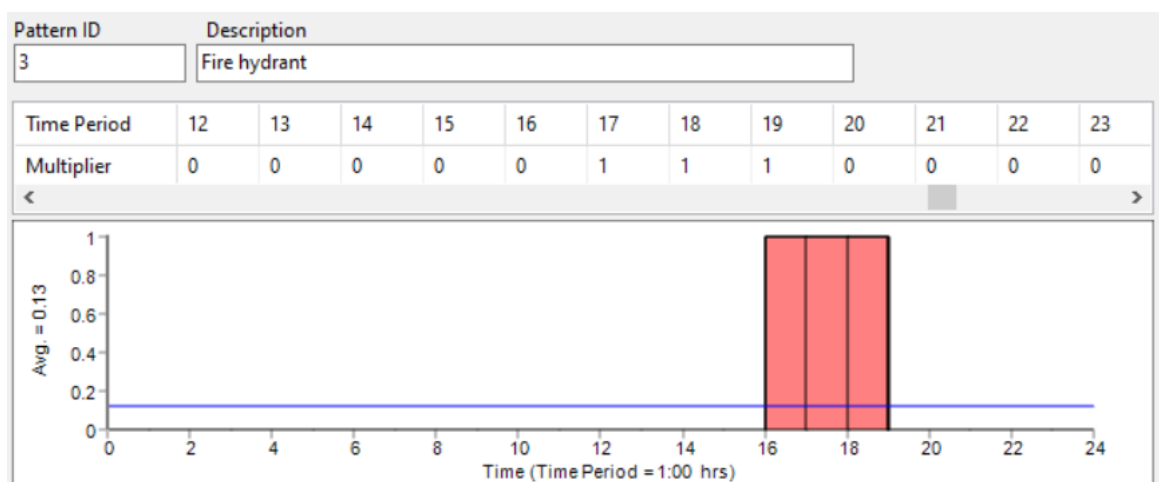
## Appendix 4: Pattern 103 industrial use



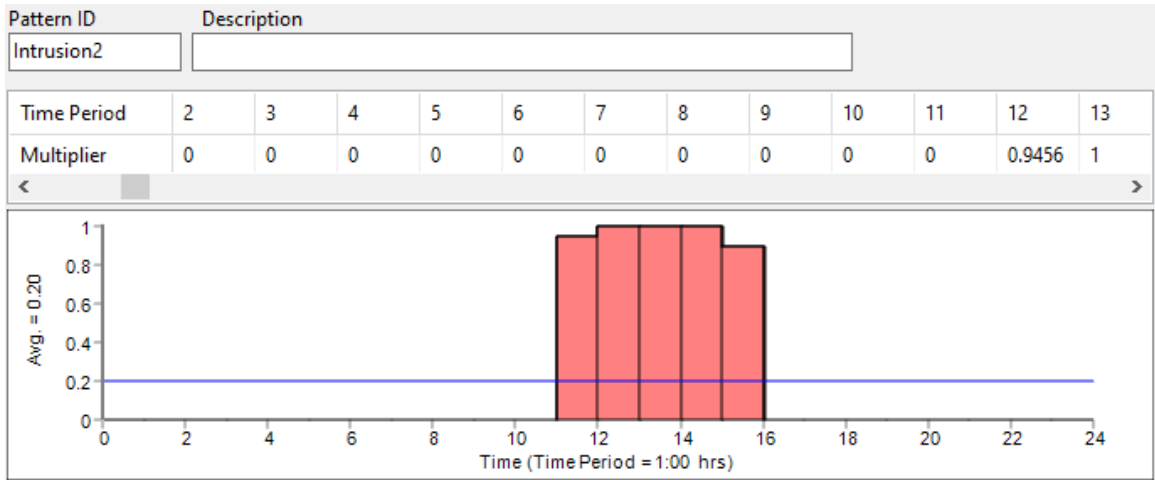
## Appendix 5: Scenario 2, pump malfunction



## Appendix 6: Scenario 3 pattern-Fire Emergency



## Appendix 7: Pathogen Intrusion pattern during pump malfunction



### Appendix 8: Pathogen Intrusion pattern during pump Emergency fire

